

Unger, V., Liebner, S., Koebisch, F., Yang, S., Horn, F., Sachs, T., Kallmeyer, J., Holger-Knorr, K., Rehder, G., Gottschalk, P., Jurasinski, G. (2021): Congruent changes in microbial community dynamics and ecosystem methane fluxes following natural drought in two restored fens. - Soil Biology and Biochemistry, 160, 108348.

<https://doi.org/10.1016/j.soilbio.2021.108348>

1 **Title**

2 Congruent changes in microbial community dynamics and ecosystem methane fluxes following
3 natural drought in two restored fens

4

5 **Author names and affiliations**

6 Viktoria Unger^a, Susanne Liebner^{b,c}, Franziska Koebsch^a, Sizhong Yang^b, Fabian Horn^b,
7 Torsten Sachs^d, Jens Kallmeyer^b, Klaus-Holger Knorr^e, Gregor Rehder^f, Pia Gottschalk^d,
8 Gerald Jurasinski^a

9 ^aLandscape Ecology and Site Evaluation, Faculty of Agricultural and Environmental Sciences,
10 Rostock University, 18059 Rostock, Germany

11 ^bGFZ German Research Centre for Geosciences, Helmholtz Centre Potsdam, Telegrafenberg,
12 14473 Potsdam, Germany

13 ^cUniversity of Potsdam, Institute of Biochemistry and Biology, 14476 Potsdam, Germany

14 ^dRemote Sensing and Geoinformatics, GFZ German Research Centre for Geosciences,
15 Helmholtz Centre Potsdam, Telegrafenberg, 14473 Potsdam, Germany

16 ^eEcohydrology & Biogeochemistry Group, Institute of Landscape Ecology, University of
17 Münster, 48149 Münster, Germany

18 ^fDepartment of Marine Chemistry, Leibniz Institute for Baltic Sea Research, 18119
19 Warnemünde, Germany

20

21 **Author contributions**

22 VU and SL formulated the research questions and study design. VU, SL, FK, and GJ performed
23 the fieldwork. VU performed the lab work. FH and SY conducted the bioinformatic analyses.
24 FK and PG processed the eddy covariance flux data. JK and KHK provided equipment for
25 geochemical analyses and aided in geochemical data acquisition and preparation. VU, GJ, SL,

26 SY, FK, and TS prepared the figures. VU prepared the original paper draft. All authors
27 contributed to the interpretation and discussion of the data, as well as writing of the paper.

28

29 **Key words**

30 Drought; Methane; Fen; Peatland; Methanogens; Methanotrophs

31

32 **Abstract**

33 Both the frequency and intensity of drought events are expected to increase, with unresolved
34 alterations to peatland methane cycling and the involved microbial communities. While existing
35 studies have assessed drought effects via experimental approaches under controlled conditions,
36 to our knowledge, no studies have examined the *in-situ* effects of natural drought in restored
37 temperate fens. In this study, we used quantitative polymerase chain reaction (qPCR) and high
38 throughput 16S rRNA gene amplicon sequencing of DNA and complementary DNA (cDNA)
39 to determine the abundances and community structure of total and putatively active microbial
40 communities following the 2018 European summer drought. Together with geochemical and
41 methane flux data, we compared these results to a non-drought reference dataset. During
42 drought, water level and methane flux rates decreased to a new recent minimum in both fens.
43 This corresponded with pronounced shifts in porewater geochemistry. Microbial community
44 composition in the drought year differed markedly, and was characterized by a greater relative
45 and total abundance of aerobic methanotrophs, and, in one of the two sites, by a decrease in
46 total methanogen abundance. In contrast to the non-drought reference years, type I
47 methanotrophs were clearly more dominant than type II methanotrophs in both fens. cDNA
48 sequencing confirmed the activity of type I methanotrophs during drought, with
49 *Methylomonaceae* having the highest average relative abundance of bacterial cDNA transcripts.
50 We show that changes in microbial community dynamics, porewater geochemistry, and
51 ecosystem methane fluxes can be substantial following natural drought in restored fens, and

52 provide the first *in-situ* evidence from a natural drought which suggests type I methanotroph
53 populations are more active than type II methanotrophs in response to drought effects. Type I
54 methanotrophs may represent a key microbial control over methane emissions in restored
55 temperate fens subject to natural drought.

56

57 **1 Introduction**

58 Peatlands, which store a substantial portion of the world's terrestrial organic carbon (approx.
59 550 to 1,055 Gt; Yu et al., 2010; Nichols and Peteet 2019), also emit a globally significant
60 amount of the greenhouse gas methane (CH₄; Bastviken et al., 2011). Peatland ecosystems are
61 particularly vulnerable to drought events, which are likely to increase in frequency and intensity
62 in the upcoming decades (Laiho 2006; IPCC 2014). Methane in peatlands is produced
63 metabolically by methanogenic archaea (methanogens) under water-logged, reducing
64 conditions, when other terminal electron acceptors (TEAs) used in the breakdown of organic
65 matter are depleted (Froelich et al., 1979; Peters and Conrad 1996; Zehnder and Stumm 1988).
66 Methane that does not reach the atmosphere via ebullition, diffusion, or direct transport by plant
67 aerenchyma (Joabsson et al., 1999; Baird et al., 2004) may be oxidized either aerobically or
68 anaerobically by bacteria or archaea (methanotrophs). This mechanism, performed mainly by
69 aerobic methanotrophs in peatlands, can reduce CH₄ emissions substantially (Yavitt et
70 al., 1988). Drought events can decrease peatland CH₄ emissions by reducing water level and
71 altering redox geochemistry (Roden and Wetzel 1996; Knorr and Blodau 2009; Kang et al.,
72 2018). Associated community dynamics of methanogens and methanotrophs, however, are not
73 well understood. *In situ* studies of fen peatlands in this respect are scarce, (Cadillo-Quiroz et
74 al., 2008), although, compared to bogs, fens may be particularly sensitive to drying (Jaatinen et
75 al., 2007; Peltoniemi et al., 2016).

76 The activity, abundance, and community structure of microbes can be altered by drought effects
77 (Knorr et al., 2008; Kim et al., 2008; Ma et al., 2013; Potter et al., 2017). Oxidative stress can
78 decrease rates of CH₄ production (Jasso-Chávez et al., 2015) and/or cause methanogen
79 mortality (Morozova and Wagner 2007). This is supported by incubation studies and mesocosm
80 experiments that show decreases in CH₄ production (Dowrick et al., 2006; Knorr and Blodau
81 2009) and methanogen gene abundances (Kim et al., 2008) after short term drought treatments.
82 In two field studies of peatland archaeal communities of the Tibetan plateau, Tian et al. (2012
83 and 2015) found that drought caused a 10-fold decrease in archaeal abundance (of which the
84 majority were methanogens) and altered community composition. Ma and Lu (2011) also noted
85 a significant decrease in archaeal abundance in a rice paddy soil following short-term drought
86 treatments, citing a decrease in methanogen abundance. In a field manipulation experiment,
87 Peltoniemi et al. (2016) found that both warming and drying decreased methanogen abundances
88 in boreal fens. In some studied locations, however, no changes in methanogen abundance and
89 community structure were found (e.g. Kim et al., 2008; Peltoniemi et al., 2016), suggesting
90 drought-induced changes to microbial community dynamics may differ among individual
91 peatlands.

92 Whether aerobic methanotrophic communities can maintain function under increasing
93 frequency and intensity of natural drought is still not clear (Ho et al., 2016a). Drought effects
94 on aerobic methanotrophic communities in peatlands have been studied mostly in controlled
95 incubation experiments (e.g. Henckel et al., 2001; Ma and Lu 2011; Collet et al., 2015; Ho et
96 al., 2016a; van Kruistum et al., 2018). Some aerobic methanotrophs benefit from water level
97 reduction and modest soil drying (Henckel et al., 2001; Ma and Lu 2011; Peltoniemi et al.,
98 2016). Aerobic proteobacterial methanotrophs are divided into types I (gammaproteobacteria)
99 and II (alphaproteobacteria) based on phylogenetic and biochemical distinctions (Knief 2015),

100 and an increasing number of studies suggest a differential response to drying events among
101 aerobic methanotroph types (Collet et al., 2015; Ho et al., 2016a; Peltoniemi et al., 2016).

102 Functional traits dictate microbial response to environmental changes, and determine their
103 survival strategy (i.e., life strategy; Ho et al., 2013a). Incubation studies suggest that type I
104 methanotrophs can adjust more readily to moisture and temperature fluctuations, and are able
105 to rapidly increase activity and population size once suitable conditions return (Henkel et al.,
106 2001; Bodelier et al., 2012; Ho et al., 2013a, b; Pan et al., 2014; Collet et al., 2015; Ho et al.,
107 2016a, b). Though ubiquitous in peatlands, type II methanotroph populations are thought to be
108 comparatively stable under changing temperature and moisture regimes (Henckel et al., 2001;
109 Collet et al., 2015) as a consequence of their different life strategy as stress-tolerators, compared
110 to type I methanotrophs, which have been described broadly as competitor-ruderals (Ho et al.,
111 2013a). This has not yet been investigated in fens under natural drought. However, in their field
112 manipulation experiment, Peltoniemi et al. (2016) found a combination of warming and drying
113 decreased the abundance of some type I methanotrophs, while differences in the abundance of
114 type II methanotrophs could only be explained by depth, and not by warming and/or drying
115 treatments.

116 The 2018 European drought (Hanel et al., 2018) provided the opportunity to examine microbial
117 community and CH₄ emission dynamics in a natural setting. According to the European Centre
118 for Medium-Range Weather Forecasts, the near-surface air temperature anomaly from April to
119 August 2018 in Europe was greater than in any year since 1979, with the Baltic Sea region
120 experiencing the highest anomalies (Magnusson et al., 2018). Data from the National Oceanic
121 and Atmospheric Administration place 2018 as the warmest summer in Europe on record since
122 1910 (NOAA Global Climate Report 2020). From April to September 2018, monthly
123 precipitation averaged across Germany was 25.6 % (April) to 52.7 % (July) less than the 1981-
124 2010 reference period average (Deutscher Wetterdienst 2020). Such drastic deviations are

125 likely to be reflected in fen CH₄ cycling and the involved microbial communities, but most
126 existing studies are experimental (e.g. Kim et al., 2008; Tian et al., 2015; Peltoniemi et al.,
127 2016) or do not examine methanogens and methanotrophs specifically (e.g. Tian et al., 2012).

128 Total microbial, methanogen, and methanotroph community dynamics have not yet been
129 studied together with CH₄ emissions and porewater geochemistry in restored fens affected by
130 natural drought. Therefore, during the 2018 European summer drought, we collected peat and
131 porewater samples from two previously studied fens in Northeastern Germany. We analyzed
132 peat microbial community structure and relative abundances using 16S rRNA gene sequencing,
133 and determined total microbial, methanogen, and bacterial methanotroph abundances using
134 quantitative PCR (qPCR). We include porewater geochemical analyses, as well as ongoing CH₄
135 flux and water level measurements, and compared this dataset to a similar dataset from non-
136 drought years preceding 2018 (Wen et al., 2018). In the drought year only, we employed reverse
137 transcription of total RNA and subsequent sequencing of complementary DNA (cDNA) to
138 develop a community profile of active microbes. We aimed to elucidate methanogen and
139 methanotroph community dynamics associated with decreasing CH₄ emissions in restored fens
140 affected by natural drought. Along with a decrease in CH₄ flux rates, we hypothesized a
141 decrease in the abundance of methanogens, as well as shifts in microbial community
142 composition, with a greater representation of aerobic taxa during drought, specifically
143 methanotrophs. Furthermore, we expected the community profile of microbes active during
144 drought to be dominated by aerobic taxa.

145

146 **2 Materials and Methods**

147 *2.1 Study sites*

148 For a detailed description of the study sites, see Wen et al. (2018). Briefly, the Hütelmoor is a
149 coastal minerotrophic fen of approx. 360 ha located at the Baltic Sea in NE Germany (Fig. 1a

150 and b). In the past, the fen received brackish water inflows from occasional storm surges,
151 though the last brackish water intrusion event happened more than 20 years ago, in 1995. Since
152 then, the brackish sulfate (SO_4^{2-}) pool of the upper soil horizons has been fully depleted, so that
153 contemporary conditions for CH_4 cycling correspond to those of freshwater peatlands (Koebsch
154 et al., 2019; Wen et al., 2018). Dominant vegetation at the site includes *Phragmites australis*,
155 *Bolboschoenus maritimus*, *Carex acutiformis*, and *Schoenoplectus tabernaemontani*. The
156 second site, Zarnekow, is a riparian fen of approx. 500 ha, located in the valley of the river
157 Peene in NE Germany (Fig. 1a and c). The dominant emergent macrophyte is *Typha latifolia*.
158 Both fens were drained for agricultural purposes and were restored in 2005 (Zarnekow) and
159 2010 (Hütelmoor) by permanently raising water levels above peat surface. After rewetting,
160 average CH_4 fluxes increased dramatically (Augustin and Chojnicki 2008; Hahn et al., 2015;
161 Franz et al., 2016; Wen et al., 2018). The porewater pH at both sites ranges from slightly acidic
162 to circumneutral (~6–8). Electrical conductivity in the Hütelmoor averages 5.3 mS cm^{-1}
163 compared to 1.5 mS cm^{-1} in Zarnekow.

164 **Figure 1 here, to be printed in color**

165 **Figure 1.** Location of the study sites in Northeastern Germany (a) and sampling locations in
166 the coastal fen, the Hütelmoor (b), and the riparian fen, Zarnekow (c). Two sampling points
167 were located in each of the wet unvegetated (WU) and dry unvegetated (DU) subsites. Aerial
168 images were taken in May 2018, before average water levels decreased in the fens.

169 2.2 Peat and porewater collection (drought year)

170 Peat and porewater samples for the drought year were collected on August 30 and September
171 12, 2018 in the Hütelmoor and Zarnekow, respectively. At this time, the average water level in
172 both fens was visibly lower, nevertheless, the distinct microtopography led to a patchy mosaic
173 of dry spots, and small ponds with water depths ~10 cm or less. Samples were collected in both
174 the dry and wet subsites to assess whether spatial patterns in hydrology led to larger differences

175 in microbial community dynamics and geochemistry than drought. Sampling was conducted in
176 non-vegetated sites to exclude the potential influence of plants and rhizosphere effects on CH₄
177 cycling and involved microorganisms. In each subsite, duplicate peat cores were collected for
178 analyses of microbial community composition and concentrations of dissolved CH₄ and carbon
179 dioxide (CO₂). Surface samples were collected for microbial analyses only. A third and fourth
180 core (one from each subsite) were collected for bulk density and porewater geochemical
181 analyses, respectively. All peat cores were semi-cylindrical (5 cm width x 50 cm depth) and
182 were collected with a Russian D-corer (De Vleeschouwer et al., 2010). The cores were split
183 into 10 cm depth sections and the depth sections 0-10, 20-30, and 40-50 cm were analyzed for
184 this study.

185 Peat samples for microbial analyses were collected using sterile equipment, placed in 15 ml
186 Falcon Tubes and immediately placed in a dry-shipper that was pre-cooled with liquid nitrogen.
187 Samples were stored in the lab at -80 °C for approximately one week until nucleic acid
188 extraction. For dissolved CH₄ and CO₂ concentrations and their ¹³C/¹²C isotopic composition,
189 a 3 ml peat “plug” was collected with a tip-cut 3 ml syringe from each depth section and placed
190 in a 20 ml vial containing 5M NaCl solution. The vials were closed immediately with butyl
191 rubber stoppers and aluminum crimp caps with no headspace, and then stored upside down until
192 processing. After collecting a peat plug of a known volume for bulk density analysis (again
193 using a tip-cut syringe), peat samples for porewater geochemical analyses were immediately
194 packed in air-tight aluminum bags and sealed with plastic clips. Upon returning to the lab
195 several hours later, the aluminum bags were flushed with nitrogen gas, completely degassed
196 using a vacuum pump, heat-sealed, and stored at 4°C until analysis.

197 Sampling during the drought year could not be conducted at the exact same time points as
198 sampling in the non-drought year due to the inability to anticipate the onset and duration of
199 drought events. However, previous work in the fens, and similar fens from the same region,

200 revealed little variation in key parameters considered in the present study among late summer
201 and early autumn. Monthly porewater sampling campaigns conducted June through November
202 (2015) in both fens showed minimal variation in dissolved oxygen, SO_4^{2-} , nitrate (NO_3^-), and
203 nitrite (NO_2^-) concentrations. The porewater data were published in Wen et al. (2018) but were
204 not presented in a monthly fashion. Additionally, preliminary (unpublished) research in the
205 Hütelmoor showed no significant differences in qPCR-based methanogen and methanotroph
206 abundances among the summer and autumn seasons. No such data are available for Zarnekow,
207 however, given that site conditions typically do not change drastically between July and mid-
208 September, any temporal influence should be negligible compared to the effects of the extreme
209 drought. Finally, Wang et al. (2021) found no seasonal variation in prokaryotic microbial
210 community composition in other coastal and riparian fen systems in northeastern Germany.

211 *2.3 Sample and data collection (non-drought year)*

212 A detailed description of the study design and methods from the non-drought year is provided
213 in Wen et al. (2018), but a summary of this, and an explanation how the data were applied in
214 this study, are provided here. Peat and pore water were collected in four locations in the
215 Hütelmoor and five locations in Zarnekow in October 2014 and July 2015, respectively. At the
216 time of sampling, the sampling locations were fully inundated since rewetting. From this
217 timepoint, two sampling locations from each fen were selected to compare to the data collected
218 in the drought year. This was done to ensure that data from similar locations in the fens were
219 compared.

220 In both the drought and non-drought years, peat collection methods for microbial analyses were
221 conducted with the same equipment and analyzed with the same protocols. Porewater collection
222 differed between the drought and non-drought years. In the non-drought year, porewater was
223 collected from permanently installed porewater dialysis samplers using a syringe. In the
224 drought year, peat samples were collected, from which porewater was extracted using a

225 hydraulic pore water press. Dissolved CH₄ and dissolved CO₂ concentrations were determined
226 using the same equipment, while concentrations of TEAs and isotopic analyses were conducted
227 on different equipment. Sequencing data from the non-drought year were initially analyzed and
228 published using OTU clustering methods (Wen et al., 2018). For the present study, amplicon
229 sequence variant methods were employed, and sequencing data from the non-drought year were
230 therefore reanalyzed accordingly. RNA extraction, reverse transcription, and subsequent cDNA
231 sequencing were conducted in the drought year only.

232 *2.4 Water level and methane flux measurements*

233 Water level in Zarnekow was derived with a sonic ranging sensor SR50A (Campbell Scientific,
234 Canada) that measured the distance from a fixed platform down to the water surface. The
235 distance measured by the SR50A was corrected for temperature effects and converted to water
236 levels relative to the sediment surface. Water level in the Hütelmoor was derived from pressure
237 transducers using a HOBO 13-Foot Depth Titanium Water Level Data Logger (Onset, Bourne,
238 USA) after barometric pressure correction, and was referenced to the mean surface level. In
239 this study, water levels below the peat surface are denoted with a negative sign.

240 Methane fluxes were measured with the eddy covariance approach, which provides a
241 continuous time series of half-hourly gas fluxes on ecosystem scale. In the Hütelmoor, the
242 measurement setup comprised of two open-path infrared gas analyzers (LI-7500 and LI-7700,
243 both LI-COR, Lincoln, NE, USA), and a three-dimensional sonic anemometer (CSAT3,
244 Campbell Scientific, Logan, UT, USA) for wind velocities and sonic temperature. All signals
245 were recorded by a CR3000 Micrologger (Campbell Scientific, Logan, UT) with a scan rate of
246 10 Hz. In Zarnekow, the setup for CH₄ flux measurements comprised of an open-path CH₄
247 analyzer (LI-7700, LI-COR, Lincoln, NE, USA) and a closed-path Fast Greenhouse Gas
248 Analyzer (FGGA EP, Los Gatos Research). The sonic anemometer is a Gill HS-50 (Gill,
249 Lymington, Hampshire, UK) and raw data were recorded with a LI-7550 digital data logger

250 system (LI-COR Biogeosciences, Lincoln, NE, USA) at 20 Hz in half-hourly files. Though
251 instrumentation and configuration differed slightly between both sites, each of the measurement
252 setups is well in line with the default practice used for eddy covariance-determined greenhouse
253 gas flux measurements (for details see Koebisch et al. 2020). Half-hourly net CH₄ fluxes were
254 processed with the software EddyPro version 6.0.0 (LI-COR, Lincoln, NE, USA). Data gaps
255 were imputed with the same artificial neural network approach for both sites.

256 *2.5 Bulk density and porewater chemistry*

257 Water content was determined by dividing the oven dry weight of a given peat sample over the
258 wet weight. Bulk density (g dry weight cm⁻³) of each depth section was calculated by dividing
259 the oven dry weight of a peat sample by the initial volume. Porewater for geochemical (pH and
260 anion) analyses was extracted from the peat samples using an IODP-style titanium pore water
261 squeezer (Manheim 1966) in a 22-ton hydraulic press (Carver, Wabash, USA). The extractors
262 were fitted with 0.22 µm pore size filters. Anions (NO₂⁻, NO₃⁻, and SO₄²⁻) were quantified on
263 an ion chromatograph system with an S5200 sample injector, a 3.0 mm×150 mm SykroGel A
264 01 column, a S3115 conductivity detector (all SYKAM Chromatographie Vertriebs GmbH,
265 Germany), and a SeQuant SAMS anion IC suppressor (Merck KGaA, Germany). The eluent
266 (6 mM Na₂CO₃ and 90 µM NaSCN) had a flow rate of 1 mL min⁻¹. Column oven temperature
267 was 50 °C, and the injection volume was 50 µl.

268 *2.6 Dissolved methane and carbon dioxide*

269 In the lab, a 3 mL gas headspace was created in each porewater sample vial by addition of
270 ultrapure helium using two sterile syringes. After being allowed to equilibrate for two weeks
271 (upside down to avoid gas leakage) samples were analyzed on a 7890A gas chromatograph
272 (GC) system (Agilent Technologies, Germany) equipped with a flame ionization detector and
273 a Carboxen PLOT Capillary Column or HP-Plot Q (Porapak-Q) column. Injection volume was
274 250 µL. Dissolved CH₄ and CO₂ concentrations were calculated and converted to micromolar

275 values from the equation $\frac{G*H}{T*R*V*P} * 1000$, where G = headspace gas mole fraction (ppm), H =
276 headspace volume (3 mL), T = absolute temperature (301.15 °K), R = universal gas constant
277 (0.082 L·atm·K⁻¹·mol⁻¹), V = peat volume (3 mL), and P = peat porosity. Porosity was
278 calculated from the measured bulk density.

279 *2.7 Isotopic composition of methane and carbon dioxide*

280 The ¹³C/¹²C isotopic composition of CH₄ and CO₂ was determined using cavity ring-down
281 spectroscopy (CRDS; PICARRO G2201-i PICARRO Instruments, Sunnyvale, CA, United
282 States) coupled to a Small Sample Isotope Module (SSIM) in order to measure small gas sample
283 volumes (~20 ml). To avoid interference with hydrogen sulfide present in samples, 1 ml of a
284 saturated Zn-acetate solution was added to precipitate hydrogen sulfide as ZnS. As the
285 measurement range of the instrument is 300-2000 ppm for CO₂ and 2.5-2000 ppm CH₄, small
286 gas samples from headspace vials were taken (100 µL) and analyzed on a GC equipped with
287 FID and TCD (GC 2010, Shimadzu, Kyoto, Japan) to determine a suitable dilution in synthetic
288 air for isotope measurements. The calibration for CH₄ was performed using a working standard
289 of 1000 ppm (-42.48 ‰) and four standards of 2500 ppm (-38.30, -54.45, -66.50 and -69.00
290 ‰). CO₂ calibration was performed using a standard of 1000 ppm with known isotopic
291 signature of -31.07 ‰ and dilution of pure CO₂ with signatures of -27.10 and -4.55 ‰,
292 respectively. All gas standards had been calibrated against reference materials from IAEA
293 (RM8562) using elemental analysis coupled to isotope ratio mass spectrometry (EA 3000,
294 Eurovector, Redavalle, Italy; Horizon, NU Instruments, Wrexham, UK) or were provided from
295 Air Gas (Air Liquide, Plumsteadville, PA, USA) or from Isometric Instruments (GASCo,
296 Victoria, BC, Canada) with certificates. Isotope values are expressed in units of per mill (‰)
297 in the typical δ-notation vs. V-PDB.

298 *2.8 DNA extraction and sequencing*

299 Genomic DNA was extracted from 150 to 200 mg of peat soil per sample using an EurX
300 GeneMATRIX soil DNA Purification Kit. DNA concentrations were quantified using a
301 Nanophotometer P360 (Implen GmbH, Munich, Germany). Polymerase chain-reaction (PCR)
302 analysis of bacterial and archaeal 16S rRNA genes was performed as detailed in Wen et al.
303 (2018). Primer combinations for archaea were S-D-Arch-0349-a-S-17/S-D-Arch-0786-a-A-20
304 (Takai and Horikoshi 2000) and S-D-Bact-0341-b-S-17/S-D-Bact-0785-a-A-21 (Herlemann et
305 al., 2011) for bacteria. The targeted amplicons were a length of 400 for bacteria and 406 for
306 archaea. Illumina HiSeq sequencing was performed by Eurofins Genomics using 300 bp paired-
307 end mode and a 20 % PhiX Control v3 library to offset the effects of low-diversity sequence
308 libraries.

309 *2.9 RNA extraction and cDNA synthesis*

310 Total RNA was extracted using the Qiagen RNeasy PowerSoil Total RNA kit. The resulting
311 RNA was purified using a TURBO DNA-free kit (Invitrogen). Complete digestion of DNA was
312 verified using RNA as non-template control in conventional 16S rRNA PCR reactions as
313 described in Liebner and Svenning (2013). Quality of the RNA was checked with an Agilent
314 2100 Bioanalyzer (Agilent Technologies, US). Reverse Transcriptase polymerase chain
315 reaction was conducted on total RNA according to in house protocol. First, 10 µl sterile distilled
316 water, 1 µl 10mM dNTP mix (Invitrogen), 1 µl pd(N)₆ Random Hexamer (GE Healthcare), and
317 1 µl of sample were combined in a PCR tube on ice (final volume 13 µl). The mixture was
318 heated at 65°C for 5 minutes in a PCR machine (Bio-Rad) and immediately chilled on ice. The
319 contents of the tubes were spun down and the following reagents were then added: 1 µl sterile
320 distilled water, 1 µl M DTT, 1 µl Superscript III Reverse Transcriptase (Invitrogen), and 4 µl 5
321 x First Strand Buffer. The reagents were mixed gently by pipetting up and down, and were
322 incubated first at 25°C for 5 minutes (because random primers were used), then 50°C for 60
323 minutes, and finally deactivated by heating at 70°C for 15 minutes. The resulting cDNA was

324 then used as a template for PCR amplification. PCR amplification was performed on bacterial
325 and archaeal cDNA using the same primer combinations as mentioned above.

326 2.10 *Taxonomic analyses*

327 Cutadapt (Martin 2011) was used to demultiplex the NGS libraries. Primer sequences were
328 detected while allowing for a maximum error rate of 10 % whereas sample barcodes were not
329 allowed to show any sequencing error while having a high-quality score (Q25). The DADA2
330 pipeline (Callahan et al., 2016) was applied to process the sample sequence libraries by
331 truncating (250 bp forward reads; 200 bp reverse reads) and filtering read sequences. A library-
332 specific error model was generated and used for dereplication, for sample inference and for the
333 merging of read pairs. Resulting sequences were required to have a minimum length of 200 bp
334 and their orientation was standardized by calculating the hamming distance of the sequences
335 and their reverse complements. De novo chimera removal was applied to the resulting sequence
336 table. The resulting amplicon sequence variants (ASVs) were assigned to the SILVA taxonomy
337 (v132) (Quast et al., 2013) by applying vsearch (Rognes et al., 2016) as implemented in the
338 QIIME2 pipeline (Bolyen et al 2018). In order to account for different sequencing depths, the
339 relative abundances of the ASVs were used for the visualization and comparison of the
340 microbial communities.

341 2.11 *Quantification of 16S rRNA, mcrA, and pmoA gene copy numbers*

342 Quantitative polymerase chain reaction (qPCR) was performed on a Bio-Rad CFX instrument
343 (Bio-Rad, Munich, Germany) using the SYBR green method for determination of 16S *rRNA*
344 (total bacterial), *mcrA* (methanogenic), and *pmoA* (bacterial methanotrophic) gene copy
345 numbers. Technical replicates were performed in triplicate. A detailed description of the
346 procedure can be found in Wen et al. (2018). *Methylocella* spp. were not present in the
347 sequencing data and the marker gene *mmoX* was therefore excluded from qPCR analysis.

348 2.12 *Statistical methods and data visualization*

349 All statistics and data visualization were done using R (R Core Team 2019). The Mann-Whitney
350 test was employed to examine differences in geochemical parameters and microbe abundances
351 in drought versus non-drought years, as well as subsites. To assess whether the 2018 drought
352 led to a significant reduction in CH₄ flux rates, daily individual CH₄ fluxes across the years
353 2015–2018 were compared using Tukey’s honest significance (Tukey’s HSD) test. This
354 analysis was conducted for CH₄ flux rates over (i) the entire year, (ii) a subperiod of March–
355 November, and (iii) a subperiod of September–December. The full results of the analyses are
356 provided in the supplemental data (Fig. S1). Means, maximums, and sums of CH₄ fluxes for
357 each time period were calculated and are also provided in the supplemental material (Table S1,
358 S2). Additionally, correlation analyses were performed for CH₄ fluxes and water level,
359 precipitation, and air temperature. For air temperature, a fitted exponential model was
360 constructed, and correlation coefficients were determined. NMDS ordinations were constructed
361 using the function metaMDS of R package vegan (Oksanen et al., 2019) to visualize
362 dissimilarity in microbial community composition at the family level among subsites and before
363 and after drought. Bubble plots were constructed at the family level to examine differences in
364 relative abundances of methanogens and methanotrophs between drought and non-drought
365 conditions, as well as to visualize the active communities of both groups. In the bubble plots,
366 family level is presented in order to remain consistent with previously published sequencing
367 data from the two sites.

368 2.13 *Accession numbers*

369 The 16S rRNA gene sequence data from the non-drought year were deposited at EBI under the
370 BioProject PRJNA356778. The Hütelmoor sequence read archive accession numbers are
371 SRR5118134 - SRR5118155 and SRR5119428 - SRR5119449 for bacterial and archaeal
372 sequences, respectively. The Zarnekow accession numbers are SRR6854018 - SRR6854033
373 and SRR6854205 - SRR6854220 for bacterial and archaeal sequences, respectively. Raw
374 sequencing data from the drought year are available at the European Nucleotide Archive under

375 BioProject accession number PRJEB38162 and sample accession number ERS4542720-
376 ERS4542857.

377 **3 Results**

378 *3.1 Methane emissions and water level*

379 Methane emissions and water level dynamics were similar among the fens in the drought year
380 (Fig. 2). Water levels were high in April 2018, at 0.6 and 0.8 m above the surface in the
381 Hütelmoor and Zarnekow, respectively (Fig. 2c and d). However, water levels dropped steadily
382 from May on and reached surface level between end of July/beginning of August. At this time,
383 CH₄ emissions in both fens peaked at 0.90 (Hütelmoor) and 0.87 (Zarnekow) g m⁻² d⁻¹, then
384 decreased sharply afterwards (Fig. 2a and b). For the rest of the year, CH₄ emissions remained
385 low with median fluxes of 0.02 and 0.04 g m⁻² d⁻¹, respectively. Although water levels rose
386 above ground surface in November, CH₄ emissions were lower than the same time period of
387 the three previous years. This held particularly for the Hütelmoor, where median November
388 CH₄ fluxes reached only 3% of the magnitude of the previous 3 reference years.

389 *Figure 2 here -to be printed in black and white*

390 **Figure 2.** Annual trends in eddy covariance-determined methane flux rates (a and b) and water
391 level (c and d) for the Hütelmoor and Zarnekow. Grey areas represent the range of measured
392 values for the three years prior to the drought year (2015 - 2017), while the solid black line
393 represents the drought-year average (2018). Dotted lines indicate the time of sampling in the
394 drought year.

395 Methane flux rates in the drought year differed from all other years in both fens ($p < 0.05$) only
396 when comparing the subperiod of September to December 2018 (Supplemental data, Fig S1)
397 when the drought effects were most prominent (Fig. 2). When considering the entire year, CH₄
398 emissions in the drought year were significantly lower compared to 2015 and 2016, in the
399 Hütelmoor only, with no statistically significant differences in Zarnekow.

400 **Figure 3 here - to be printed in color**

401 Figure 3. Fitted exponential models for CH₄ flux rates (g m⁻² day⁻¹) versus air temperature (°C)
402 in the Hütelmoor (a) and Zarnekow (b) fen peatlands in NE Germany. Solid lines represent
403 average values, while shaded areas delineate 95% confidence intervals. Orange and blue colors
404 correspond to the time periods of January – August and September – December in the three
405 years prior to the drought (2015-2017), respectively. Red and black colors correspond to the
406 time periods of January – August and September – December in the drought year (2018),
407 respectively. Calculated correlation coefficients are shown for each time period within the
408 panels.

409 Methane fluxes did not correlate with precipitation or water level (data not shown), but there
410 was a distinct exponential temperature response (Fig. 3), which weakened during and after the
411 drought. Correlation coefficients calculated for September – December in 2018, the time period
412 during and immediately after the drought, were lower (Fig. 3).

413 3.2 Porewater geochemistry

414 Dissolved SO₄²⁻ concentrations were higher during drought in both fens ($p = 0.02$, Table 1),
415 while NO₃⁻ concentrations did not differ among the drought and non-drought years ($p > 0.05$).
416 In contrast to the non-drought year, where NO₃⁻ was only detected in a few surface samples,
417 NO₃⁻ was detected in nearly every sample during drought. Dissolved CH₄ concentrations were
418 significantly lower in both fens during the drought (Table 1). Dissolved CO₂/CH₄ ratios were
419 higher in the dry subsites than wet subsites, ranging from 31 to 1,912 and 1 to 18 in dry and
420 wet subsites respectively (Table 1). δ¹³C-CH₄ values ranged from -67.5‰ to -52.5‰ Slightly
421 higher δ¹³C-CH₄ values were measured in the dry subsites of Hütelmoor (-52.5‰) and
422 Zarnekow (-56.7‰) at the 20-30 and 40-50 cm depths, respectively. Except for the 0-10 cm
423 depth in the Hütelmoor and 40-50 cm depth in Zarnekow, where δ¹³C-CO₂ values were -13.3‰
424 and -14.8‰, respectively, δ¹³C-CO₂ values in the dry subsites were around -20‰. In the wet

425 subsites, $\delta^{13}\text{C-CO}_2$ values were higher (Table 1). Gas concentrations were too low to determine
426 isotopic values for depths of 0 to 40 cm in the dry subsites in Zarnekow, and isotopic values for
427 the 40 to 50 cm depth section in Zarnekow could only be obtained for one core (Table 1).

428 **Table 1.** Total microbial, methanogen, and methanotroph abundances as well as geochemical
429 parameters for dry and wet subsites during the 2018 summer drought. Values shown are
430 averages calculated from duplicate cores.

	Depth	16S rRNA	<i>mcrA</i>	<i>pmoA</i>	Dissolved CH ₄	Dissolved CO ₂	CO ₂ /CH ₄	δ ¹³ C-CH ₄	δ ¹³ C-CO ₂	NO ₃ ⁻	NO ₂ ⁻	SO ₄ ²⁻
	cm	copies g dry peat ⁻¹	copies g dry peat ⁻¹	copies g dry peat ⁻¹	μM	μM		V-PDB	V-PDB	mM	mM	mM
Hütelmoor Dry	Surface	3.6 x 10 ¹⁰	6.5 x 10 ⁸	4.8 x 10 ⁷	-	-	-	-	-	-	-	-
	0-10	2.0 x 10 ¹⁰	7.2 x 10 ⁸	2.7 x 10 ⁷	8	1194	121	-60.9	-21.0	6.20	-	28.5
	20-30	1.2 x 10 ¹⁰	2.0 x 10 ⁸	1.1 x 10 ⁷	12	1147	94	-52.5	-21.6	-	-	19.0
	40-50	1.3 x 10 ¹⁰	1.0 x 10 ⁸	9.2 x 10 ⁶	6	739	69	-63.3	-19.6	3.51	2.75	35.7
Hütelmoor Wet	Surface	2.2 x 10 ¹⁰	1.5 x 10 ⁹	1.2 x 10 ⁸	-	-	-	-	-	-	-	-
	0-10	3.3 x 10 ¹⁰	8.7 x 10 ⁸	7.8 x 10 ⁷	248	1818	5	-64.6	-13.3	0.03	0.09	0.60
	20-30	2.6 x 10 ¹⁰	3.0 x 10 ⁶	2.7 x 10 ⁷	80	777	17	-66.3	-19.8	0.12	0.15	0.44
	40-50	8.9 x 10 ⁹	4.2 x 10 ⁶	7.5 x 10 ⁶	35	1231	18	-67.5	-20.9	3.57	0.22	38.6
Zarnekow Dry	Surface	2.0 x 10 ¹⁰	1.6 x 10 ⁸	3.6 x 10 ⁷	-	-	-	-	-	-	-	-
	0-10	2.2 x 10 ¹⁰	2.4 x 10 ⁸	1.5 x 10 ⁷	0.4	1072	1912	-	-	0.09	0.12	1.49
	20-30	1.8 x 10 ¹⁰	1.2 x 10 ⁸	2.3 x 10 ⁷	4	1080	276	-	-	0.19	0.20	1.16
	40-50	7.3 x 10 ⁹	4.5 x 10 ⁷	8.5 x 10 ⁶	27	666	31	-56.7	-14.8	0.10	0.07	0.33
Zarnekow Wet	Surface	1.8 x 10 ⁹	1.2 x 10 ⁸	1.0 x 10 ⁷	-	-	-	-	-	-	-	-
	0-10	3.7 x 10 ¹¹	6.1 x 10 ⁷	8.5 x 10 ⁶	538	332.4	1	-62.5	-10.2	-	-	0.65
	20-30	3.2 x 10 ¹⁰	4.4 x 10 ⁷	7.1 x 10 ⁶	382	651.0	1	-65.0	-10.8	0.53	0.38	33.90
	40-50	5.5 x 10 ¹⁰	4.9 x 10 ⁶	2.9 x 10 ⁶	226	667.4	6	-62.9	-13.2	-	-	2.25

432 3.3 16S *rRNA*, *mcrA*, and *pmoA* gene copy numbers

433 During drought, total microbial abundance based on 16S *rRNA* gene copy numbers ranged from
434 1.8×10^9 to 3.7×10^{11} and was—compared to the non-drought year—slightly higher in
435 Zarnekow ($p = 0.03$), but did not differ in the Hütelmoor (Table 1). Total methanogen
436 abundance based on *mcrA* gene copy numbers ranged from 3.0×10^6 to 1.5×10^9 copies g dry
437 peat⁻¹ and was significantly lower in Zarnekow during drought ($p = 9.8 \times 10^{-5}$), but similar
438 among the drought and non-drought years in the Hütelmoor ($p = 0.4$). Total bacterial
439 methanotroph abundance based on *pmoA* gene copy numbers, which ranged from 2.9×10^6 to
440 1.2×10^8 copies g dry peat⁻¹, was significantly higher in the Hütelmoor during the drought ($p =$
441 2.5×10^{-2}) but did not differ in Zarnekow ($p = 0.15$). Bacterial methanotroph abundances were
442 significantly higher in the dry subsites in Zarnekow ($p = 0.007$), but no other significant
443 differences in gene abundances were found among dry and wet subsites.

444 3.4 Overall community composition of bacteria and archaea

445 According to the NMDS ordination, bacterial community composition based on 16S *rRNA* gene
446 sequencing differed among the fens in both the drought and non-drought years (Fig. 4). In the
447 drought year, bacterial community composition differed from the non-drought year in
448 Zarnekow. In the Hütelmoor, surface sample bacterial community composition clearly differed
449 among the drought and non-drought year, but there was some similarity among the deeper
450 samples. The patterns of differentiation were not consistent among the fens, with community
451 composition diverging in Zarnekow and converging in the Hütelmoor. Expectedly, surface
452 samples showed the strongest differentiation in community composition among drought and
453 non-drought years. Archaea community composition also differed among the fens at both time
454 points (Fig. 4). Community composition converged strongly in the Hütelmoor following
455 drought, but there was little overall difference among the dry and wet subsites and time points.
456 In Zarnekow, archaeal community composition during drought clearly differed from the non-

457 drought year. Notably, the relative abundances of the phyla Actinobacteria and Firmicutes were
458 higher in both fens during drought (data not shown).

459 **Figure 4 here, to be printed in color**

460 **Figure 4.** NMDS ordinations showing bacterial (a) and archaeal (b) community composition
461 in the non-drought year (pre WU) and the wet and dry subsites of the drought-year (post WU
462 and post DU, respectively). Points represent distinct microbial communities, with the darkest
463 points representing the microbial community composition at depth (40 – 50 cm), and the lightest
464 points representing surface sample communities. Polygons indicate clusters within the
465 respective time points. The dotted and dashed polygons refer to samples from the drought-year,
466 while the solid polygons refer to the non-drought year. Blue highlights samples from the
467 Hütelmoor (HM) and yellow highlights samples from Zarnekow (ZN).

468 *3.5 Methanotroph community composition and relative abundances based on 16S rRNA gene*
469 *sequencing and cDNA sequencing*

470 In contrast to the non-drought year, the type I aerobic methanotrophs of the order
471 Methylococcales clearly dominated the methanotrophic community during drought. Type I
472 methanotrophs of Methylococcales were detected in all but four samples, and represented an
473 average of 1.1 % of total bacterial community, with a maximum of 3 % in dry subsites, and 6
474 % in wet subsites. In particular, there was a pronounced increase in the distribution and relative
475 abundance of family *Methylomonaceae*, but *Methylococcaceae* were also detected in a greater
476 number of samples in the drought year (Fig. 5 a and b). The distribution and abundance of type
477 II methanotrophs within *Beijerinckiaceae* was similar among the drought and non-drought
478 years (Fig. 5 a and b). *Methylomonas* was the most abundant genus, followed by *Crenothrix*,
479 *Methylobacter*, *Methylococcus*, “*Candidatus Methylospira*”, and *Methyloparacoccus*. Type II
480 methanotrophs were represented mainly by *Methylocystis*, and were only a small portion of the
481 *Beijerinckiaceae* taxa detected, making up only 0.1 % of bacterial community or less.

482 *Methylomirabilaceae*, the family containing proposed anaerobic methanotroph (ANME)
483 “*Candidatus Methylomirabilis*” (*Ca. Methylomirabilis*), was detected in many samples from
484 both time points (Fig. 5 a and b), and was represented almost exclusively by the uncultured
485 group Sh765B-TzT-35. *Ca. Methylomirabilis* was detected in deeper peat (20–50 cm depth) at
486 both time points in Zarnekow where it represented 0.01 to 0.05 % of bacterial community, but
487 was low in abundance (≤ 0.05 %) and not detected in the Hütelmoor (data not shown).

488 **Figure 5 here, to be printed in color**

489 **Figure 5.** Bubble plots showing the relative abundances (in %) of aerobic methanotrophs (blue),
490 methanogens (red), and ANME (orange) for the non-drought (a) and drought years (b and c).
491 Plots a and b were constructed from sequenced DNA in the non-drought and drought year,
492 respectively, while plot c was constructed from sequenced cDNA from the drought-year only.
493 The abundances shown for aerobic methanotrophs are calculated relative to total bacterial
494 community, while the abundances of methanogens and ANME are calculated relative to total
495 archaeal community. Sequencing data are shown for the family level. Other groups besides
496 methanogens and methanotrophs that may be classified within the shown groups are not
497 included in this chart.

498 Along with other aerobic bacteria (e.g. *Arenicellaceae* and *Nitrosomondaceae*), type I
499 methanotrophs (mostly *Methylomonaceae*) were active during drought, and dominated the
500 active community profile (Supplemental data, Fig. S3). Within the bacterial community, type I
501 methanotrophs of *Methylomonaceae* had the highest average (8 %) and maximum (26 %) relative
502 abundance of all methanotrophs (Fig. 5 c). Type II methanotrophs (*Methylocystis*) were
503 active in just five samples from both fens, with a maximum relative abundance of 0.09 % of
504 bacteria. *Ca. Methylomirabilis* was detected in just two deeper samples in Zarnekow. However,
505 *Methylomirabilaceae*, and in particular group Sh765B-TzT-35 (data not shown), represented a
506 significant portion of the cDNA-determined community (Fig. 5 c).

507 In the DNA-based community profile, the archaeal ANME family *Methanoperedencaceae* was
508 detected in nearly all depths in both fens, but was relatively most abundant in deeper peat (Fig.
509 5 a and b). This family was represented entirely by the anaerobic methanotroph “*Candidatus*
510 *Methanoperedens nitroreducens*” (*Ca. M. nitroreducens*). At depths of 20 to 50 cm, “*Ca. M.*
511 *nitroreducens*” represented up to 2 % of archaea in the Hütelmoor and up to 18 % in Zarnekow.
512 In the active community profile, “*Ca. M. nitroreducens*” was detected in one sample from
513 Hütelmoor at 40 – 50 cm, where it represented 0.2 % of archaeal cDNA sequences. In
514 Zarnekow, it was detected at 40 – 50 cm in both cores from the dry subsites with relative
515 abundances of 0.4 and 4 % (Fig. 5). This was additionally the only location and depth where
516 “*Ca. Methyloirabilis*” (group Sh765B-TzT-35) cDNA sequences were detected. The
517 organism is understood to use NO_2^- produced by “*Ca. M. nitroreducens*” via anaerobic CH_4
518 oxidation coupled to NO_3^- reduction (Ettwig et al., 2010; Haroon et al., 2013).

519

520 3.6 Methanogen community composition and relative abundances based on DNA and cDNA 521 sequencing

522 In the drought year, methanogens remained the most abundant archaeal group, along with
523 Crenarchaeota (Supplemental data, Fig. S4). During drought, *Methanosaetaceae* accounted for
524 23 – 97 % of archaeal community in the DNA-based, which was similar to relative abundances
525 measured in the non-drought year (Fig. 5 a and b). The acetoclastic methanogens
526 *Methanosaetaceae* (also known as *Methanothrix*) dominated the archaeal community, along
527 with the metabolically diverse *Methanosarcinaceae*, the H_2 /formate-utilizing
528 *Methanoregulaceae*, and the hydrogenotrophic *Methanomassiliicoccaceae* (Supplemental data,
529 Fig. S4). This was also reflected in the active community profiles (Fig. 5 c; Supplemental data,
530 Fig. S5). Taxa that were detected in the DNA-based community profiles were not always
531 detected in the active community profiles at similar depths (this was true for both bacteria and

532 archaea), suggesting the presence of inactive microorganisms (Fig. 5 a – c, Supplemental data,
533 Figs. S2–S5).

534

535 **4 Discussion**

536 *4.1 Drought methane emissions and site conditions*

537 In both fens, a substantial peak in CH₄ emissions occurred in August of the drought year, as
538 water level approached the peat surface. The magnitude of the peak exceeded CH₄ emission
539 rates of the previous 3 years (Fig. 2). Previous studies have reported a brief pulse in CH₄
540 emissions associated with water level reduction in peatlands, likely because of degassing due
541 to reduced hydrostatic pressure (Moore et al., 1990; Dinsmoore et al., 2009) and/or increasing
542 peat temperatures associated with the heat wave, as warming can enhance CH₄ production
543 significantly as long as fen peats are moist (Turetsky et al., 2008). In the present study, CH₄
544 emissions correlated strongly with temperature, but not water level or precipitation (Fig. 3).
545 Once water levels reached below the peat surface, CH₄ emissions were diminished (below 0.2
546 g CH₄ m⁻² d⁻¹), and a decoupling of CH₄ emissions and temperatures occurred, as indicated by
547 calculated correlation coefficients (Fig. 3). This is likely due to the increasing importance of a
548 combination of other factors in regulating CH₄ emissions from the investigated sites, such as
549 oxygen intrusion related to increased diffusivity upon water level decline, and changes in
550 microbial community dynamics.

551 Despite increasing water levels in autumn, CH₄ emissions remained low in both fens (Fig. 2),
552 and were significantly lower in the time period of September to December, compared to the
553 previous 3 years (Supplemental data, Fig. S1, Tables S1, S2), signifying a biogeochemical
554 legacy of draining. This could be explained by drought-induced reoxidation of alternative TEAs
555 (Estop-Aragonés et al., 2013; Clark et al., 2020). During drought, we measured higher SO₄²⁻
556 concentrations and detected NO₃⁻ at greater depths and in a larger number of samples compared

557 to the non-drought year. With these (and other) alternative electron acceptors, various other
558 microorganisms may outcompete methanogens for substrates (Kristjansson and Schönheit
559 1983; Scholten et al., 2002; Gao et al., 2019), effectively inhibiting methanogenesis. In the
560 Hütelmoor, the drought-related decrease in CH₄ emissions led to lower yearly CH₄ emissions
561 in 2018, compared to the years 2015 and 2016, while no differences were found in annual CH₄
562 budgets in Zarnekow (Supplemental data, Fig. S1, Tables S1, S2). This nevertheless highlights
563 the potential for drought events to lead to significant reduction in CH₄ emissions, and may
564 translate to changes in CH₄ budgets on a broader scale (e.g., regional budgets). However,
565 compilation of data from various sites is needed to venture into regional or global predictions,
566 as highlighted by the contrasting results from our two study sites.

567 At the time of sampling during the drought year, CH₄ emissions had already dropped to a new
568 recent minimum, and the shifting site conditions were evident in the geochemical data. During
569 drought we measured (mostly in the dry subsites) significantly lower dissolved CH₄
570 concentrations, high dissolved CO₂/CH₄ ratios, as well as more negative $\delta^{13}\text{C-CO}_2$ values
571 (Table 1). High CO₂/CH₄ ratios indicate CO₂ formation from other metabolic processes such
572 as aerobic decomposition, reduction of alternative TEAs, or CH₄ oxidation (Corbett et al., 2013;
573 Holmes et al., 2015; Gao et al., 2019), while CO₂/CH₄ ratios close to one are associated with
574 predominantly methanogenic conditions (Keller et al., 2009). CO₂ produced from non-
575 methanogenic pathways should have a $\delta^{13}\text{C-CO}_2$ signature closer to the parent organic matter,
576 as observed in the dry subsites or during drought (with two exceptions, Table 1), while CO₂
577 produced via methanogenesis is enriched in ¹³C, as observed under wet conditions (Boehme et
578 al., 1996 ; Corbett et al., 2013 ; Table 1). With respect to the measured $\delta^{13}\text{C-CO}_2$ values,
579 contribution of older CO₂ and CO₂ formed at depth cannot be excluded. Nevertheless, together,
580 the geochemical data show a shift in redox conditions and associated dominating metabolic
581 pathways, and underscore the more oxidized site conditions under drought. This is supported

582 by our taxonomic dataset that shows a shift toward the dominance of aerobic bacteria.
583 Additionally, the relative abundances of phyla Actinobacteria and Firmicutes were higher
584 during drought (data not shown). Studies of the root-associated microbiome of grasses (Naylor
585 et al., 2017) and rice (Santos-Medellín et al., 2017) have also noted an increase in the relative
586 abundance of these groups following experimental drought manipulations.

587 Though average water level decrease was not as dramatic in Zarnekow during the drought (Fig.
588 2), we conclude the drought-induced water level reduction was a major contributor to the
589 patterns observed in this study. In the non-drought years, average water level was at or above
590 the peat surface by September (the time of sampling in the drought year). During the drought
591 year, water level remained below the surface late into autumn. The heat wave during the drought
592 year probably exacerbated the effects of the water level decrease, as widespread drying out of
593 the peat surface was observed, in contrast to previous years. A separate study of the same sites
594 showed that water level decrease in both fens stressed the established vegetation, and led to
595 changes in vegetation composition and atmospheric carbon exchange (Koebsch et al. 2020).
596 Similarities in CH₄ emission trajectories (Fig. 2), porewater geochemistry (Table 1), and
597 aspects of microbial community composition among the two fens during the drought year
598 further support the conclusion that water level decrease led to the observed patterns.

599 *4.2 Total microbial abundances and community structure*

600 Differences in gene abundances and microbial community structure between the drought and
601 non-drought years were site-specific. We expected to detect a lower total abundance of
602 methanogens in both fens due to lowering of average water level and potential associated
603 oxidative stress, as has been documented in previous studies of fen peat (Tian et al., 2012; Tian
604 et al., 2015; Peltoniemi et al., 2016). In the present study, total methanogen abundance was
605 significantly lower following drought compared to a non-drought year in the riparian fen
606 (Zarnekow), but no difference was found in the coastal fen (Hütelmoor). Methanotroph

607 abundance was significantly higher in the coastal fen, while in the riparian fen, total
608 methanotroph abundance was greater only in the dry subsites sampled. This observation is
609 likely due to differing site conditions of the fens, differing initial microbial community
610 compositions, and/or stress history of the microbial communities within them. In a mesocosm
611 study, Kim et al. (2008) found that short-term drought treatments decreased methanogen
612 abundance in bog, but not in fen peats. Based on this and other evidence, they concluded that
613 distinct microbial communities associated with different peatland types would respond
614 differently to drought effects. Other studies echo this conclusion (Jaatinen et al., 2007; Ho et
615 al., 2016b; Peltoniemi et al., 2016).

616 Environmental stress history is important in shaping microbial communities, as stress selects
617 for taxa that are able to withstand disturbances (Ho et al., 2016b; Krause et al., 2018; van
618 Kruistum et al., 2018). Although both fens in this study were historically drained for agricultural
619 purposes, microbial communities in the Hütelmoor may be better adapted to environmental
620 stress, having experienced fluctuating salinity and water levels associated with historical
621 seawater intrusions. Baumann and Marschner (2013) suggested that microorganisms tolerant to
622 salt stress are likely more resistant to desiccation, though the study did not examine CH₄-
623 cycling microbes specifically. Overall, these results show that a months-long, natural drought
624 can change the total abundance of methanogens and methanotrophs, and support previous
625 studies that suggest abundance patterns may differ among individual peatlands.

626 The ordination analyses further illustrate how patterns in microbial community dynamics may
627 vary among individual peatlands. Microbial community composition differed among the fens,
628 as has often been reported in previous studies (Kim et al., 2008; Peltoniemi et al., 2016; Wen
629 et al., 2018). In this study, this was true for both the drought and non-drought years. Community
630 composition (including both wet and dry subsites) of bacteria and archaea during drought was
631 distinct from community composition under inundated conditions, with the exception of a few

632 deeper samples that showed some overlap, and of archaea in the Hütelmoor (Fig. 4). Based on
633 this and the qPCR results, the archaeal community in Zarnekow appeared to be more strongly
634 affected by the drought than in the Hütelmoor. This is in line with some long-term studies that
635 indicate drought will alter bacterial and archaeal community composition (Tian et al., 2012;
636 Tian et al., 2015). Other studies suggest that archaeal community composition may be more
637 resistant to warming and/or drying effects in both the short- and long-term (Kim et al., 2008;
638 Peltoniemi et al., 2016). Although archaea community composition converged strongly in the
639 Hütelmoor in the drought year, there was little separation among the polygons indicating the
640 different time points (Fig. 4 b), suggesting less change in community composition. It is
641 worthwhile to highlight that, while changes in methanogen and methanotroph abundances and
642 overall microbial community composition differed among the fens, CH₄ emission dynamics
643 were ultimately similar, implying functional redundancy among microbial groups. Peltoniemi
644 et al. (2016) reported a similar observation, when they found CH₄ emission dynamics to be
645 similar among two fens subject to warming and drying treatments, despite differing patterns in
646 microbial control over the emissions.

647 4.3 *Methanotroph relative abundances and links to laboratory studies*

648 According to 16S *rRNA* gene sequencing, the increase in the relative abundance of type I
649 aerobic methanotrophs, in particular *Methylomonaceae*, was striking in both fens (Fig. 5 a and
650 b). In the Hütelmoor, type I methanotrophs were hardly detectable in the non-drought year (Fig.
651 5). Previously, it was believed that type II methanotrophs may be more resistant to drought
652 stress due to formation of desiccation-resistant spores (Whittenbury et al., 1970; Bowman
653 2006). However, more recent work has shown type I methanotrophs to be unexpectedly
654 resistant to environmental stress, as well as responsive to fluctuations in temperature and water
655 availability (Collet et al., 2015; Ho et al., 2016b), while type II methanotroph populations,
656 though ubiquitous, are relatively stable and do not experience significant changes in population

657 size in comparison. To our knowledge, Peltoniemi et al. (2016) were the first to provide *in situ*
658 evidence of this in fens. They found type I methanotroph abundances were altered by warming
659 and drying treatments, while depth was the only controlling factor over type II methanotrophs.
660 Similarly, in our study, there was little difference in the distribution and relative abundance of
661 type II methanotrophs between the drought and non-drought years.

662 This study provides the first *in situ* evidence from a natural drought that suggests type I
663 methanotrophs are comparatively adaptive to changes in temperature and water availability,
664 which supports earlier experimental work (Henkel et al., 2001; Ho et al., 2013a; Ho et al.,
665 2013b; Pan et al., 2014; Collet et al., 2015; Ho et al., 2016a; Ho et al., 2016b; Peltoniemi et al.,
666 2016). The dominance of type I methanotrophs during drought was confirmed by cDNA
667 sequencing. The type I methanotrophs of the *Methylomonaceae* family had the highest relative
668 amount of cDNA transcripts (Fig. 5), and were one of the most abundant bacterial groups
669 (Supplemental data, Fig. S3). Thus, type I methanotrophs may represent a significant microbial
670 control over CH₄ emissions in restored temperate fens subject to natural drought.

671 4.4 Evidence for anaerobic methanotrophic activity

672 Denitrifying anaerobic methanotrophs “*Ca. M. nitroreducens*” (archaea) and “*Ca.*
673 *Methylomirabilis*” (bacteria) were detected in both the DNA- and cDNA-based community
674 profiles at the same depths. Interestingly, at these depths, the highest $\delta^{13}\text{C}$ -CH₄ values were
675 measured (20 – 30 and 40 – 50 cm depths), and higher $\delta^{13}\text{C}$ values (approaching -50‰) in
676 dissolved CH₄ may be indicative of CH₄ oxidation. While this is not conclusive evidence that
677 these organisms contribute to CH₄ emission mitigation in these systems, they appear to be
678 active at depth and may represent an additional filter for CH₄ produced in deeper peats. “*Ca.*
679 *M. nitroreducens*” has been implicated in CH₄ oxidation in incubations of rice paddy soils,
680 which typically have high nitrogen availability (Vaksmas et al., 2016). Decades of agricultural
681 use (and therefore increased nitrogen availability) during drainage could have promoted the

682 establishment of these organisms in the fens. The role of ANME in fens warrants further
683 investigation. In vitro studies of various peatland types suggest ANME may be capable of
684 oxidizing a significant portion of produced CH₄ (Zhu et al., 2012; Miller et al., 2019).

685

686 **5 Conclusions**

687 This study shows that reduced CH₄ emissions in drought-affected fens are associated with
688 multiple substantial changes in pore water chemistry and microbial community dynamics, and
689 that some changes in microbial community dynamics may be site-specific. In the riparian fen
690 (Zarnekow), total methanogen abundance decreased and methanotroph abundance increased in
691 some areas, while, in the coastal fen (Hütelmoor), only total methanotroph abundances
692 increased. Reduced CH₄ emissions in restored fens subject to natural drought are thus at least
693 partially the result of the differential controlling patterns of methanogens and methanotrophs.
694 However, a large increase in the relative abundance of methanotrophs, particularly type I
695 methanotrophs, was documented in both fens. We provide the first *in situ* evidence from a
696 natural drought that suggests type I methanotrophs are comparably more adaptive than type II
697 methanotrophs when experiencing drought effects. The abundance of type I methanotrophs
698 seems to be an important microbial control over CH₄ emissions in temperate fens experiencing
699 natural drought.

700

701 **6 Acknowledgements**

702 This work was funded by the DFG (Deutsche Forschungsgemeinschaft) within the framework
703 of the Research Training Group “Baltic TRANSCOAST” (GRK 2000/1). This is Baltic
704 TRANSCOAST publication no. GRK2000/002X. This study was supported by the Helmholtz
705 Gemeinschaft (HGF) by funding the Helmholtz Young Investigators Group of Susanne Liebner
706 (VH-NG-919) and Torsten Sachs (grant VH-NG-821), and by the Terrestrial Environmental
707 Observatories (TERENO) Network. The study was further funded by the European Social Fund

708 (ESF) and the Ministry of Education, Science, and Culture of Mecklenburg-Western Pomerania
709 within the scope of the project WETSCAPES (grants ESF/14-BM-A55-0030/16 and ESF/14-
710 BM-A55-0031/16). We thank Oliver Burckhardt, Anke Saborowski, and Victoria Tietz for their
711 support in the lab. We thank J. Axel Kitte for aiding in both field and lab work. We thank
712 Christian Wille for his work maintaining the Zarnekow eddy covariance tower and processing
713 the raw data. We thank Joachim Hofman for maintaining the Hütelmoor eddy covariance tower.

714

715 **Conflict of interest:**

716 The authors declare that they have no conflict of interest.

717

718 **7 References**

719 Augustin J., Chojnicki B. (2008). Austausch von klimarelevanten Spurengasen, Klimawirkung
720 und Kohlenstoffdynamik in den ersten Jahren nach der Wiedervernässung von degradiertem
721 Niedermoorgrünland (Exchange of climate relevant trace gases, climate effect and carbon
722 dynamics in the first years after rewetting of degraded fen grassland). In: Gelbrecht, J., Zak, D.
723 & Augustin, J. (eds.) Phosphor- und Kohlenstoff- Dynamik und Vegetationsentwicklung in
724 wiedervernässten Mooren des Peenetales in Mecklenburg-Vorpommern (Phosphorus and carbon
725 dynamics and vegetation development in re-wetted peatland of the Peene valley in
726 Mecklenburg-Western Pomerania). Leibniz-Institut für Gewässerökologie und
727 Binnenfischerei, Berlin, 50–67 (in German).

728

729 Baird A.J., Beckwith C.W., Waldron S., Waddington J.M. (2004). Ebullition of methane-
730 containing gas bubbles from near-surface *Sphagnum* peat. *Geophysical Research Letters*, 31,
731 L21505. doi: 10.1029/2004GL021157

732

733 Bastviken D., Tranvik L.J., Downing J.A., Crill P.M., Enrich-Prast A. (2011). Freshwater
734 methane emissions offset the continental carbon sink. *Science*, 331(6013), 50. doi:
735 10.1126/science.1196808
736
737 Baumann K., Marschner P. (2013). Effects of salinity on microbial tolerance to drying and
738 rewetting. *Biogeochemistry*, 112, 71-80. doi: 10.1007/s10533-011-9672-1
739
740 Bodelier P.L.E., Bär-Gilissen M.-J., Meima-Franke M., Hordijk K. (2012). Structural and
741 functional response of methane-consuming microbial communities to different flooding
742 regimes in riparian soils. *Ecology and Evolution*, 2(1), 106-127. doi: 10.1002/ece3.34
743
744 Boehme S.E., Blair N.E., Chanton J.P., Martens C.S. (1996). A mass balance of ¹³C and ¹²C in
745 an organic-rich methane-producing marine sediment. *Geochimica et Cosmochimica Acta*,
746 60(20), 3835-3848. doi: 10.1016/0016-7037(96)00204-9
747
748 Bolyen E., Rideout J.R., Dillon M.R., Bokulich N.A., Abnet C., Al-Ghalith G.A., Alexander
749 H., Alm E.J., Arumugam M., Asnicar F., Bai Y., Bisanz J.E., Bittinger K., Brejnrod A.,
750 Brislawn C.J., Brown C.T., Callahan B.J., Caraballo-Rodríguez A.M., Chase J., Cope E., Da
751 Silva R., Dorrestein P.C., Douglas G.M., Durall D.M., Duvallet C., Edwardson C.F., Ernst M.,
752 Estaki M., Fouquier J., Gauglitz J.M., Gibson D.L., Gonzalez A., Gorlick K., Guo J., Hillmann
753 B., Holmes S., Holste H., Huttenhower C., Huttley G., Janssen S., Jarmusch A.K., Jiang L.,
754 Kaehler B., Kang K.B., Keefe C.R., Keim P., Kelley S.T., Knights D., Koester I., Kosciulek T.,
755 Kreps J., Langille M.G., Lee J., Ley R., Liu Y., Loftfield E., Lozupone C., Maher M., Marotz
756 C., Martin B.D., McDonald D., McIver L.J., Melnik A.V., Metcalf J.L., Morgan S.C., Morton
757 J., Naimey A.T., Navas-Molina J.A., Nothias L.F., Orchanian S.B., Pearson T., Peoples S.L.,
758 Petras D., Preuss M.L., Pruesse E., Rasmussen L.B., Rivers A., Robeson II M.S., Rosenthal P.,

759 Segata N., Shaffer M., Shiffer A., Sinha R., Song S.J., Spear J.R., Swafford A.D., Thompson
760 L.R., Torres P.J., Trinh P., Tripathi A., Turnbaugh P.J., Ul-Hasan S., van der Hooft J.J., Vargas
761 F., Vázquez-Baeza Y., Vogtmann E., von Hippel M., Walters W., Wan Y., Wang M., Warren
762 J., Weber K.C., Williamson C.H., Willis A.D., Xu Z.Z., Zaneveld J.R., Zhang Y., Zhu Q.,
763 Knight R., Caporaso J.G. (2018). QIIME 2: Reproducible, interactive, scalable, and extensible
764 microbiome data science. *PeerJ Preprints*, 6 :e27295v2. doi: 10.7287/peerj.preprints.27295v2
765
766 Bowman J.P. (2006). The methanotrophs - the families Methylococcaceae and
767 Methylocystaceae, *PRO 5*, 266–289.
768
769 Callahan B., McMurdie P.J., Rosen M., Han A.W., Johnson A.J.A., Holmes S.P. (2016).
770 DADA2: High-resolution sample inference from Illumina amplicon data. *Nature Methods*, 13,
771 581-583. doi: 10.1038/nmeth.3869
772
773 Cadillo-Quiroz H., Yashiro E., Yavitt J.B., Stephen H., Zinder S.H. (2008). Characterization of
774 the Archaeal Community in a Minerotrophic Fen and Terminal Restriction Fragment Length
775 Polymorphism-Directed Isolation of a Novel Hydrogenotrophic Methanogen. *Applied and*
776 *Environmental Microbiology*, 74(4), 2059-2068. doi: 10.1128/AEM.02222-07
777
778 Clark M.G., Humphreys E.R., Carey S.K. (2020). Low methane emissions from a boreal
779 wetland constructed on oil sand mine tailings. *Biogeosciences*, 17, 667–682, doi: 10.5194/bg-
780 17-667-2020
781
782 Collet S., Reim A., Ho A., Frenzel P. (2015). Recovery of paddy soil methanotrophs from long
783 term drought. *Soil Biology & Biochemistry*, 88, 69-72. doi: 10.1016/j.soilbio.2015.04.016
784

785 Corbett J.E., Tfaily M.M., Burdige D.J., Cooper W.T., Glaser P.H., Chanton J.P. (2013).
786 Partitioning pathways of CO₂ production in peatlands with stable carbon isotopes.
787 Biogeochemistry, 114, 327-340. doi: 10.1007/s 10533-012-9813-1
788

789 De Vleeschouwer F., Chambers F.M., Swindles G.T. (2010). Coring and sub-sampling of
790 peatlands for palaeoenvironmental research. Mires and Peat, 7, 1-10.
791

792 Deutscher Wetterdienst. (2020) Climate and Environment Monthly Description. retrieved on
793 May 26, 2020 from
794 [https://www.dwd.de/EN/ourservices/klimakartendeutschland/klimakartendeutschland_monats](https://www.dwd.de/EN/ourservices/klimakartendeutschland/klimakartendeutschland_monatsbericht.html?nn=519080)
795 [bericht.html?nn=519080](https://www.dwd.de/EN/ourservices/klimakartendeutschland/klimakartendeutschland_monatsbericht.html?nn=519080)
796

797 Dinsmore K.J., Skiba U.M., Billett M.F., Rees R. M. (2009). Effect of water table on
798 greenhouse gas emissions from peatland mesocosms. Plant and Soil, 318(1-2), 229-242. doi:
799 10.1007/s11104-008- 9832-9
800

801 Dowrick D.J., Freeman C., Lock M.A., Reynolds B. (2006). Sulphate reduction and the
802 suppression of peatland methane emissions following summer drought. Geoderma, 132(3-4),
803 384-390. doi: 10.1016/j.geoderma.2005.06.003
804

805 Estop-Aragonés C., Knorr K.-H., Blodau, C. (2013). Belowground in situ redox dynamics and
806 methanogenesis recovery in a degraded fen during dry-wet cycles and flooding.
807 Biogeosciences, 10, 421–436. doi: 10.5194/bg-10-421-2013
808

809 Ettwig K.F., Butler M.K., Le Paslier D., Pelletier E., Mangenot S., Kuypers M.M.M., Schreiber
810 F., Dutilh B.E., Zedelius J., de Beer D., Gloerich J. (2010). Nitrite-driven anaerobic methane
811 oxidation by oxygenic bacteria. *Nature*, 464 (7288), 543–548. doi:10.1038/nature08883
812

813 Franz D., Koebsch F., Larmanou E., Augustin J., Sachs T. (2016). High net CO₂ and CH₄
814 release at a eutrophic shallow lake on a formerly drained fen. *Biogeosciences*, 13, 3051-3070.
815 doi: 10.5194/bg-13-3051-2016
816

817 Froelich P.N., Klinkhammer G.P., Bender M.L., Luedtke N.A., Heath G.R., Cullen D., Dauphin
818 P., Hammond D., Hartman B., Maynard V. (1979). Early oxidation of organic matter in pelagic
819 sediments of the eastern equatorial Atlantic: suboxic diagenesis. *Geochimica et Cosmochimica*
820 *Acta* 43, 1075-1090. doi: 10.1016/0016-7037(79)90095-4
821

822 Gao C., Sander M., Agethen S., Knorr K.-H. (2019) Electron accepting capacity of dissolved
823 and particulate organic matter control CO₂ and CH₄ formation in peat soils. *Geochimica et*
824 *Cosmochimica Acta*, 245, 266-277. doi: 10.1016/j.gca.2018.11.004
825

826 Hahn J., Köhler S., Glatzel S., Jurasinski G. (2015). Methane Exchange in a Coastal Fen in the
827 First Year after Flooding - A Systems Shift. *PLOS ONE* 10(10): e0140657. doi:
828 10.1371/journal.pone.0140657
829

830 Hanel M., Rakovec O., Markonis Y., Máca P., Samaniego L., Kyselý J., Kumar R. (2018)
831 Revisiting the recent European droughts from a long-term perspective. *Scientific Reports*, 8:
832 9499. doi: 10.1038/s41598-018-27464-4
833

834 Haroon M.F., Hu S., Shi Y., Imelfort M., Keller J., Hugenholtz P., Yuan Z., Tyson G.W. (2013).
835 Anaerobic oxidation of methane coupled to nitrate reduction in a novel archaeal lineage. *Nature*
836 500 (7464), 567–570. doi:10.1038/nature12375.
837
838 Henckel T., Jäckel U., Conrad R. (2001). Vertical distribution of the methanotrophic
839 community after drainage of rice field soil. *FEMS Microbiology Ecology*, 34, 279-291. doi:
840 10.1111/j.1574-6941.2001.tb00778.x.
841
842 Herlemann D.P., Labrenz M., Jürgens K., Bertilsson S., Waniek J.J., Andersson A.F. (2011).
843 Transitions in bacterial communities along the 2000 km salinity gradient of the Baltic Sea,
844 *ISME J.*, 5, 1571–1579, doi: 10.1038/ismej.2011.41
845
846 Ho A., Kerckhof F.M., Luke C., Reim A., Krause S., Boon N., Bodelier P.L.E. (2013a).
847 Conceptualizing functional traits and ecological characteristics of methane- oxidizing bacteria
848 as life strategies. *Environmental Microbiology Reports*, 5, 335-345. doi: 10.1111/j.1758-
849 2229.2012.00370.x
850
851 Ho A., Luke C., Reim A., Frenzel P. (2013b). Selective stimulation in a natural community of
852 methane oxidizing bacteria: effects of copper on *pmoA* transcription and activity. *Soil Biology*
853 & *Biochemistry*, 65, 211-216. doi: 10.1016/j.soilbio.2013.05.027
854
855 Ho A., van den Brink E., Reim A., Krause S.M.B., Bodelier P.L.E. (2016a). Recurrence and
856 Frequency of Disturbance have Cumulative Effect on Methanotrophic Activity, Abundance,
857 and Community Structure. *Frontiers in Microbiology*, 6:1493. doi: 10.3389/fmicb.2015.01493
858

859 Ho A., Lüke C., Reim A., Frenzel P. (2016b). Resilience of (seed bank) aerobic methanotrophs
860 and methanotrophic activity to desiccation and heat stress. *Soil Biology & Biochemistry*, 101,
861 130-138. doi: 10.1016/j.soilbio.2016.07.015
862

863 Holmes M.E., Chanton J.P., Tfaily M.M., Ogram A. (2015). CO₂ and CH₄ isotope
864 compositions and production pathways in a tropical peatland. *Global Biogeochemical Cycles*,
865 29, 1-18. doi: 10.1002/2014GB004951
866

867 IPCC. (2014). *Climate Change 2014: Synthesis Report. Contribution of Working Groups I, II*
868 *and III to the Fifth Assessment Report of the Intergovernmental Panel on Climate Change* [Core
869 Writing Team, R.K. Pachauri and L.A. Meyer (eds.)]. IPCC, Geneva, Switzerland, 151 pp.
870

871 Jaatinen K., Fritze H., Laine J., Laiho R. (2007). Effects of short- and long-term water-level
872 drawdown on the populations and activity of aerobic decomposers in a boreal peatland. *Global*
873 *Change Biology*, 13(2), 491-510. doi: 10.1111/j.1365-2486.2006.01312.x
874

875 Jasso-Chávez R., Santiago-Martínez M.G., Lira-Silva E., Pineda E., Zepeda-Rodríguez A.,
876 Belmont-Díaz J., Encalada R., Saavedra E., Moreno-Sánchez R. (2015). Air-Adapted
877 *Methanosarcina acetivorans* Shows High Methane Production and Develops Resistance
878 against Oxygen Stress. *PLoS ONE* 10(2) : e0117331. doi : 10.1371/journal.pone.0117331
879

880 Joabsson A., Christensen T.R., Wallén B. (1999). Vascular plant controls on methane emissions
881 from northern peatforming wetlands. *Trends in Ecology and Evolution*, 14(10), 385–388. doi:
882 10.1016/s0169-5347(99)01649-3.
883

884 Kang X., Yan L., Cui L., Zhang X., Hao Y., Wu H., Zhang Y., Li W., Zhang K., Yan Z., Li Y.,
885 Wang J. (2018). Reduced Carbon Dioxide Sink and Methane Source under Extreme Drought
886 Condition in an Alpine Peatland. *Sustainability*, 10: 4285. doi: 10.3390/su10114285
887

888 Keller J.K., Weisenhorn P.B., Megonigal J.P. (2009). Humic acids as electron acceptors in
889 wetland decomposition. *Soil Biology & Biochemistry*, 41(7), 1518-1522. doi:
890 10.1016/j.soilbio.2009.04.008
891

892 Kim S.-Y., Lee S.-H., Freeman C., Fenner N., Kang H. (2008). Comparative analysis of soil
893 microbial communities and their responses to the short-term drought in bog, fen, and riparian
894 wetlands. *Soil Biology & Biochemistry*, 40, 2874-2880. doi: 10.1016/j.soilbio.2008.08.004
895

896 Knief C. (2015). Diversity and Habitat Preferences of Cultivated and Uncultivated Aerobic
897 Methanotrophic Bacteria Evaluated Based on *pmoA* as Molecular Marker. *Frontiers in*
898 *Microbiology*, 6: 1346. doi: 10.3389/fmicb.2015.01346
899

900 Knorr K.-H., Oosterwoud M.R., Blodau C. (2008). Experimental drought alters rates of soil
901 respiration and methanogenesis but not carbon exchange in soil of a temperate fen. *Soil Biology*
902 *& Biochemistry*, 40, 1781-1791. doi: 10.1016/j.soilbio.2008.03.019
903

904 Knorr K.-H., Blodau, C. (2009). Impact of experimental drought and rewetting on redox
905 transformations and methanogenesis in mesocosms of a northern fen soil. *Soil Biology &*
906 *Biochemistry*, 41(6), 1187-1198. doi:10.1016/j.soilbio.2009.02.030
907

908 Koebisch F., Winkel M., Liebner S., Liu B., Westphal J., Schmiedinger I., Spitzky A., Gehre M.,
909 Jurasinski G., Köhler S., Unger V., Koch M., Sachs T., Böttcher M.E. (2019). Sulfate

910 deprivation triggers high methane production in a disturbed and rewetted coastal peatland.
911 Biogeosciences, 16, 1937-1953. doi: 10.5194/bg-16-1937-2019
912

913 Koebsch F., Gottschalk P., Beyer F., Wille C., Jurasinski G., Sachs T. (2020). The impact of
914 occasional drought periods on vegetation spread and greenhouse gas exchange in rewetted fens.
915 Philosophical Transactions of the Royal Society B, 375: 20190685. doi:
916 10.1098/rstb.2019.0685
917

918 Krause S.M.B., Meima-Franke M., Veraart A.J., Ren G., Ho A., Bodelier P.L.E. (2018).
919 Environmental legacy contributes to the resilience of methane consumption in a laboratory
920 microcosm system. Scientific Reports, 8: 8862. doi: 10.1038/s41598-018-27168-9
921

922 Kristjansson J.K., Schönheit, P. (1983). Why do sulfate-reducing bacteria outcompete
923 methanogenic bacteria for substrates? Oecologia, 60, 264-266. doi: 10.1007/BF00379530
924

925 Laiho R. (2006). Decomposition in peatlands: Reconciling seemingly contrasting results on the
926 impacts of lowered water levels. Soil Biology & Biochemistry, 38(8), 2011-2024. doi:
927 10.1016/j.soilbio.2006.02.017
928

929 Liebner S., Svenning M.M. (2013). Environmental Transcription of *mmoX* by Methane-
930 Oxidizing Proteobacteria in a Subarctic Palsa Peatland. Applied and Environmental
931 Microbiology, 79(2), 701-706. doi: 10.1128/AEM.02292-12.
932

933 Ma K., Lu Y. (2011). Regulation of microbial methane production and oxidation by intermittent
934 drainage in rice field soil. FEMS Microbiology Ecology, 75(3), 446-456. doi: 10.1111/j.1574-
935 6941.2010.01018.x

936

937 Ma K., Conrad R., Lu Y., (2013). Dry/Wet Cycles Change the Activity and Population
938 Dynamics of Methanotrophs in Rice Field Soil. *Applied and Environmental Biology*, 79(16),
939 4932-4939. doi: 10.1128/AEM.00850-13

940

941 Magnusson L., Ferranti L., Vamborg F. (2018). Forecasting the 2018 European heatwave.
942 *ECMWF Newsletter*, 157, 4.

943

944 Manheim F.T. (1966). A hydraulic squeezer for obtaining interstitial water from consolidated
945 and unconsolidated sediments. *USGS Ref. Pap.* 550, 171–174.

946

947 Martin M. (2011). Cutadapt removes adapter sequences from high-throughput sequencing
948 reads, *EMBnet. Journal*, 17, 10–12. doi: 10.14806/ej.17.1.200, 2011.

949

950 Meyers P.A. (1994). Preservation of elemental and isotopic source identification of
951 sedimentary organic matter. *Chemical Geology*, 114, 289-302. doi: 10.1016/0009-
952 2541(94)90059-0

953

954 Miller K.E., Lai C.-T., Dahlgren R.A., Lipson D.A. (2019). Anaerobic Methane Oxidation in
955 High-Arctic Alaskan Peatlands as a Significant Control on Net CH₄ Fluxes. *Soil Systems*, 3(1),
956 7. doi: 10.3390/soilsystems3010007

957

958 Moore T., Roulet N., Knowles R. (1990). Spatial and temporal variations of methane flux from
959 subarctic/northern boreal fens. *Global Biogeochemical Cycles*, 4(1), 29-46. doi:
960 10.1029/GB004i001p00029

961

962 Morozova D., Wagner D. (2007). Stress response of methanogenic archaea from Siberian
963 permafrost compared with methanogens from nonpermafrost habitats. *FEMS Microbiology*
964 *Ecology*, 61(1), 16-25. doi: 10.1111/j.1574-6941.2007.00316.x
965

966 Naylor D., DeGraaf S., Purdom E., Coleman-Derr D. (2017). Drought and host selection
967 influence bacterial community dynamics in the grass root microbiome. *ISME J.*, 11, 2691–
968 2704. doi: 10.1038/ismej.2017.118
969

970 Nichols J.E., Peteet D.M. (2019). Rapid expansion of northern peatlands and doubled estimate
971 of carbon storage. *Nature Geoscience*, 12, 917–921. doi: 10.1038/s41561-019-0454-z
972

973 NOAA National Centers for Environmental Information, State of the Climate: Global Climate
974 Report for April 2020, published online May 2020, retrieved on May 26, 2020 from
975 <https://www.ncdc.noaa.gov/sotc/global/202004>.
976

977 Oksanen J., Blanchet F.G., Friendly M., Kindt R., Legendre P., McGlinn D., Minchin P.R.,
978 O'Hara R.B., Simpson G.L., Solymos P., Stevens M.H.H., Szoecs E., Wagner H. (2019). *vegan*:
979 Community Ecology Package. R package version 2.5-6. [https://CRAN.R-](https://CRAN.R-project.org/package=vegan)
980 [project.org/package=vegan](https://CRAN.R-project.org/package=vegan)
981

982 Pan Y., Abell G.C.J., Bodelier P.L.E., Meima-Franke M., Sessitsch A., Bodrossy L. (2014).
983 Remarkable recovery and colonization behavior of methane oxidizing bacteria in soil after
984 disturbance is controlled by methane course only. *Microbial Ecology*, 68, 259-270. doi:
985 10.1007/s00248-014-0402-9
986

987 Peltoniemi K., Laiho R., Juottonen H., Bodrossy L., Kell D.K., Minkkinen K., Mäkiranta P.,
988 Mehtätalo L., Penttilä T., Siljanen H.M.P., Tuittila E.-S., Tuomivirta T., Fritze H. (2016).
989 Responses of methanogenic and methanotrophic communities to warming in varying moisture
990 regimes of two boreal fens. *Soil Biology & Biochemistry*, 97, 144-156. doi:
991 10.1016/j.soilbio.2016.03.007
992
993 Peters V., Conrad R. (1996). Sequential reduction processes and initiation of CH₄ production
994 upon flooding of oxic upland soils. *Soil Biology & Biochemistry*, 28(3), 371-382. doi:
995 10.1016/0038-0717(95)00146-8
996
997 Potter C., Freeman C., Golyshin P.N., Ackermann G., Fenner N., McDonald J.E., Ehbair A.,
998 Jones T.G., Murphy L.M., Creer S. (2017). Subtle shifts in microbial communities occur
999 alongside the release of carbon induced by drought and rewetting in contrasting peatland
1000 ecosystems. *Scientific Reports*, 7: 11314. doi: 10.1038/s41598-017-11546-w
1001
1002 Quast C., Pruesse E., Yilmaz P., Gerken J., Schweer T., Yarza P., Peplies J., Glöckner F.O.
1003 (2013). The SILVA ribosomal RNA gene database project: improved data processing and web-
1004 based tools, *Nucleic Acids Research*, 41, D590–596, doi: 10.1093/nar/gks1219
1005
1006 R Core Team (2019). R: A language and environment for statistical computing. R Foundation
1007 for Statistical Computing, Vienna, Austria. URL <https://www.R-project.org/>.
1008
1009 Roden E.E., Wetzel R.G. (1996). Organic carbon oxidation and suppression of methane
1010 production by microbial Fe(III) oxide reduction in vegetated and unvegetated freshwater
1011 wetland sediments. *Limnology and Oceanography*, 41(8), 1733-1748.
1012

1013 Rognes T., Flouri T., Nichols B., Quince C., Mahé F. (2016). VSEARCH: a versatile open
1014 source tool for metagenomics. *PeerJ*, 4: e2584. doi: 10.7717/peerj.2584
1015

1016 Santos-Medellín C., Edwards J., Liechty Z., Nguyen B., Sundaresan V. (2017). Drought stress
1017 results in a compartment-specific restructuring of the rice root-associated microbiomes. *mBio*
1018 8:e00764-17. doi: 10.1128/mBio.00764-17
1019

1020 Scholten J.C.M., van Bodegom P.M., Vogelaar J., van Ittersum A., Roelofsen W., Stams A.J.M.
1021 (2002). Effect of sulfate and nitrate on acetate conversion by anaerobic microorganisms in a
1022 freshwater sediment. *FEMS Microbiology Ecology*, 42(3), 375-385. doi: 10.1111/j.1574-
1023 6941.2002.tb01027.x
1024

1025 Tian J., Zhu Y., Kang X., Dong X., Li W., Chen H., Wang Y. (2012). Effects of drought on the
1026 archaeal community in soil of the Zoige wetlands of the Qinghai–Tibetan plateau. *European*
1027 *Journal of Soil biology*, 52, 84-90. doi: 10.1016/j.ejsobi.2012.07.003
1028

1029 Tian J., Shu C., Chen H., Qiao Y., Yang G., Xiong W., Wang L., Sun J., Liu X. (2015).
1030 Response of archaeal communities to water regimes under simulated warming and drought
1031 conditions in Tibetan Plateau wetlands. *Journal of Soils and Sediments*, 15, 179-188. doi:
1032 10.1007/s11368-014-0978-1
1033

1034 Takai K., Horikoshi K. (2000). Rapid detection and quantification of members of the archaeal
1035 community by quantitative PCR using fluorogenic probes. *Applied and Environmental*
1036 *Microbiology*, 66, 5066–5072. doi: 10.1128/AEM.66.11.5066-5072.2000
1037

1038 Turetsky M.R., Treat C.C., Waldrop M.P., Waddington J.M., Harden J.W., McGuire A.D.
1039 (2008). Short-term response of methane fluxes and methanogen activity to water table and soil
1040 warming manipulations in an Alaskan peatland. *Journal of Geophysical Research*, 113:
1041 G00A10. doi:10.1029/2007JG000496

1042

1043 Vaksmaa, A., Lüke, C., van Alen T., Valè G., Lupotto E., Jetten M.S.M., Ettwig K.F. (2016).
1044 Distribution and activity of the anaerobic methanotrophic community in a nitrogen-fertilized
1045 Italian paddy soil. *FEMS Microbiology Ecology*, 92(12), fiw181. doi: 10.1093/femsec/fiw181

1046

1047 van Kruistum H., Bodelier P.L.E., Ho A., Meima-Franke M., Veraart A.J. (2018). Resistance
1048 and Recovery of Methane-Oxidizing Communities Depends on Stress Regime and History; A
1049 Microcosm Study. *Frontiers in Microbiology*, 9: 1714. doi: 10.3389/fmicb.2018.01714

1050

1051 Wang H., Weil M., Dumack K., Zak D., Münch D., Günther A., Jurasinski G., Blume-Werry
1052 G., Kreyling J., Urich T. (2021). Eukaryotic rather than prokaryotic microbiomes change over
1053 seasons in rewetted fen peatlands. *bioRxiv*. doi: 10.1101/2020.02.16.951285

1054

1055 Wen X., Unger V., Jurasinski G., Koebisch F., Horn F., Rehder G., Sachs T., Zak D., Lischeid
1056 G., Knorr K.-H., Böttcher M.E., Winkel M., Bodelier P.L.E., Liebner S. (2018). Predominance
1057 of methanogens over methanotrophs in rewetted fens characterized by high methane emissions.
1058 *Biogeosciences*, 15, 6519-6536. doi: 10.5194/bg-15-6519-2018

1059

1060 Whittenbury R., Davies S.L., Davey J.F. (1970). Exospores and cysts formed by methane-
1061 utilizing bacteria. *Journal of General Microbiology*, 61, 219-226. doi: 10.1099/00221287-61-
1062 2-219

1063

- 1064 Yavitt J.B., Lang G.E., Downey D.M. (1988). Potential methane production and methane
1065 oxidation rates in peatland ecosystems of the Appalachian Mountains, United States. *Global*
1066 *Biogeochemical Cycles*, 2(3), 253-268.
- 1067
- 1068 Yu Z., Loisel J., Brosseau D.P., Beilman D.W., Hunt, S.J. (2010). Global peatland dynamics
1069 since the Last Glacial Maximum. *Geophysical research letters*, 37(13), L13402. doi:
1070 10.1029/2010GL043584
- 1071
- 1072 Zehnder A.J.B., Stumm W. (1988). *Geochemistry and Biogeochemistry of anaerobic habitats.*
1073 In: A.J.B. Zehnder (Ed.), *Wiley series in ecological and applied microbiology. Biology of*
1074 *anaerobic microorganisms* (pp. 1-38). New York: Wiley.
- 1075
- 1076 Zhu B., van Dijk G., Fritz C., Smolders A.J.P., Pol A., Jetten M.S.M., Ettwig K.F. (2012).
1077 Anaerobic Oxidization of Methane in a Minerotrophic Peatland: Enrichment of Nitrite-
1078 Dependent Methane-Oxidizing Bacteria. *Applied and Environmental Microbiology*, 78(24),
1079 8657-8665. doi: 10.1128/AEM.02102-12

Supplemental Data

(a) Hütelmoor entire year					(d) Zarnekow entire year				
	diff	lwr	upr	p adj		diff	lwr	upr	p adj
2016-2015	0.02139804	-0.01012618	0.052922262	0.3003450	2016-2015	0.011341698	-0.01421481	0.03689820	0.6638840
2017-2015	-0.01759089	-0.04913667	0.013954885	0.4780980	2017-2015	0.001531912	-0.02404207	0.02710589	0.9986975
2018-2015	-0.03727024	-0.06883767	-0.005702802	0.0129951	2018-2015	0.004518714	-0.02105527	0.03009269	0.9687702
2017-2016	-0.03898893	-0.07051315	-0.007464711	0.0081546	2017-2016	-0.009809786	-0.03536629	0.01574672	0.7567516
2018-2016	-0.05866828	-0.09021417	-0.027122384	0.0000113	2018-2016	-0.006822984	-0.03237949	0.01873352	0.9022117
2018-2017	-0.01967935	-0.05124678	0.011888088	0.3769631	2018-2017	0.002986802	-0.02258718	0.02856078	0.9905834

(b) Hütelmoor March–November					(e) Zarnekow March–November				
	diff	lwr	upr	p adj		diff	lwr	upr	p adj
2016-2015	0.02925793	-0.007592128	0.066107995	0.1729896	2016-2015	0.016120751	-0.01441631	0.04665781	0.5259329
2017-2015	-0.01622863	-0.053078693	0.020621430	0.6690881	2017-2015	0.003008888	-0.02752817	0.03354595	0.9942829
2018-2015	-0.04715843	-0.084008491	-0.010308368	0.0056420	2018-2015	0.005851478	-0.02468558	0.03638854	0.9606520
2017-2016	-0.04548657	-0.082336627	-0.008636504	0.0083427	2017-2016	-0.013111863	-0.04364892	0.01742520	0.6866694
2018-2016	-0.07641636	-0.113266425	-0.039566302	0.0000007	2018-2016	-0.010269273	-0.04080633	0.02026779	0.8227794
2018-2017	-0.03092980	-0.067779859	0.005920264	0.1353221	2018-2017	0.002842589	-0.02769447	0.03337965	0.9951669

(c) Hütelmoor September–December					(f) Zarnekow September–December				
	diff	lwr	upr	p adj		diff	lwr	upr	p adj
2016-2015	-0.03471091	-0.060411060	-0.009010766	0.0030412	2016-2015	-0.012644704	-0.02747245	0.0021830366	0.1250960
2017-2015	-0.01502216	-0.040722309	0.010677986	0.4341202	2017-2015	-0.011054778	-0.02588252	0.0037729626	0.2201220
2018-2015	-0.10480862	-0.130561811	-0.079055427	0.0000000	2018-2015	-0.027880208	-0.04270795	-0.0130524675	0.0000100
2017-2016	0.01968875	-0.006011395	0.045388899	0.1988906	2017-2016	0.001589926	-0.01323781	0.0164176668	0.9926169
2018-2016	-0.07009771	-0.095850897	-0.044344514	0.0000000	2018-2016	-0.015235504	-0.03006324	-0.0004077633	0.0413954
2018-2017	-0.08978646	-0.115539649	-0.064033265	0.0000000	2018-2017	-0.016825430	-0.03165317	-0.0019976893	0.0188336

Figure S1: Full results of the Tukey's Honest Significance test, conducted on daily eddy covariance-determined CH₄ fluxes (g m⁻² d⁻¹) from a coastal fen (Hütelmoor: a, b, and c) and a riparian fen (Zarnekow: d, e, and f) in northeastern Germany. The analysis was conducted for three distinct time periods within the years 2015–2017 (non-drought years) and 2018 (a drought year). The three time periods analyzed include: the entire year, March–November, and September–December. *p*-values below 0.05 indicate significantly different CH₄ fluxes among the time periods.

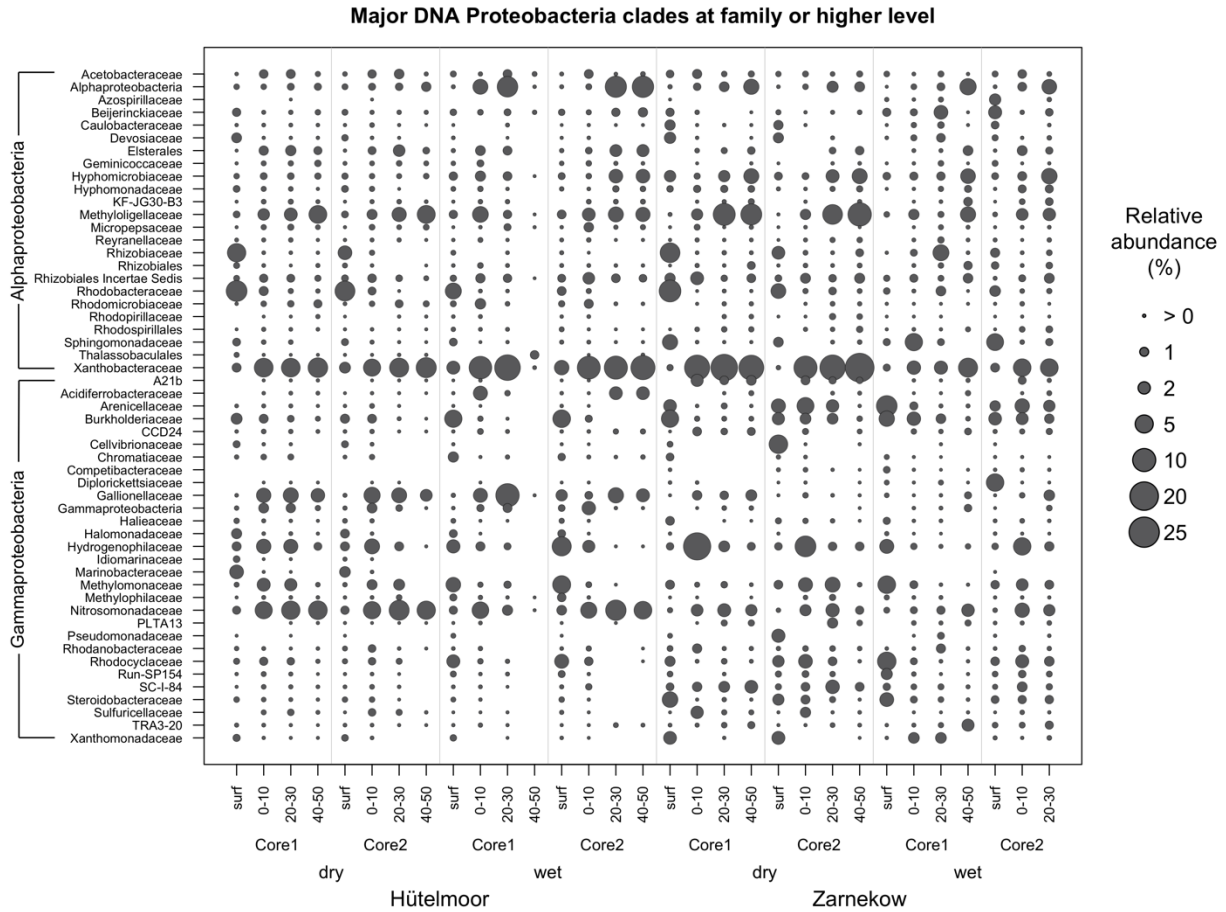


Figure S2. Bubble plots showing relative abundance of major bacterial families during the 2018 summer drought based on 16s rRNA gene sequencing. Samples are arranged along the x-axis according to site (HM and ZN for the Hütelmoor and Zarnekow, respectively) and depth section in cm (surf = surface samples) given as a range. The Abbreviations DU and WU denote samples from dry unvegetated and wet unvegetated subsites, respectively. Taxa were placed at the next possible higher taxonomic level if assignment to the family level was not possible.

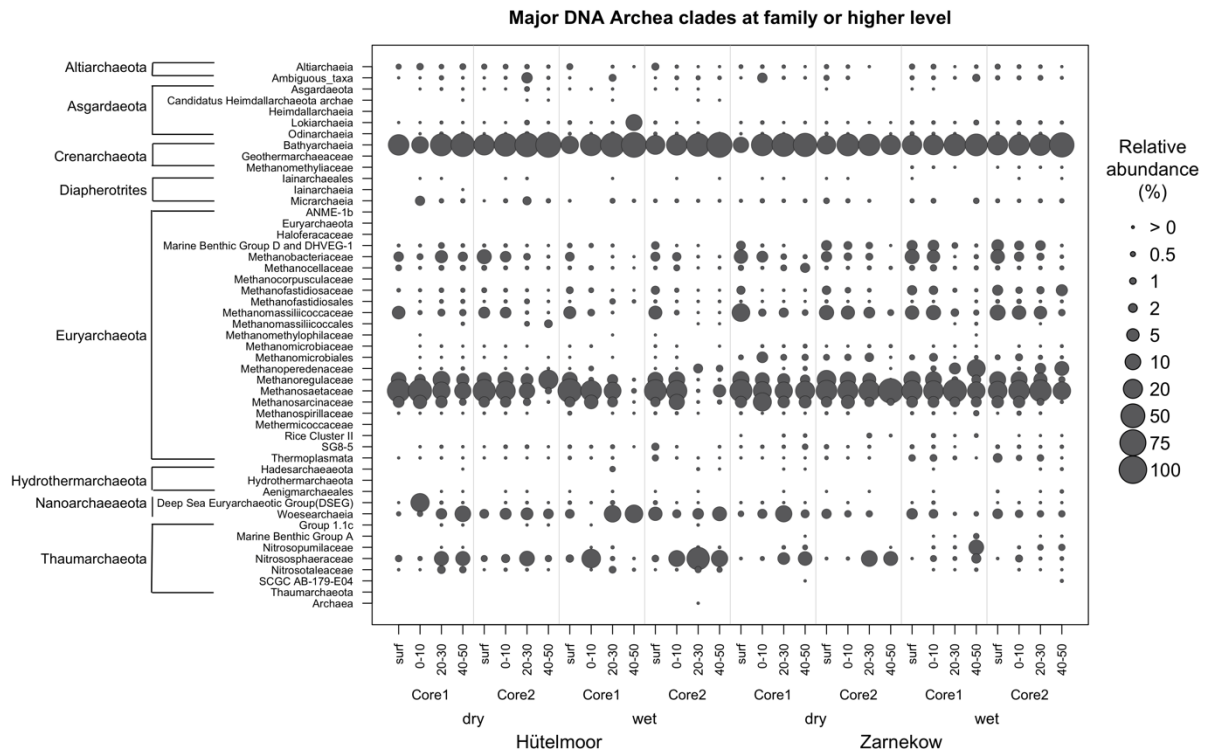


Figure S4. Bubble plots showing relative abundance of major archaeal families during the 2018 summer drought based on 16s rRNA gene sequencing. Samples are arranged along the x-axis according to site (HM and ZN for the Hütelmoor and Zarnekow, respectively) and depth section in cm (surf = surface samples) given as a range. The Abbreviations DU and WU denote samples from dry unvegetated and wet unvegetated subsites, respectively. Taxa were placed at the next possible higher taxonomic level if assignment to the family level was not possible.

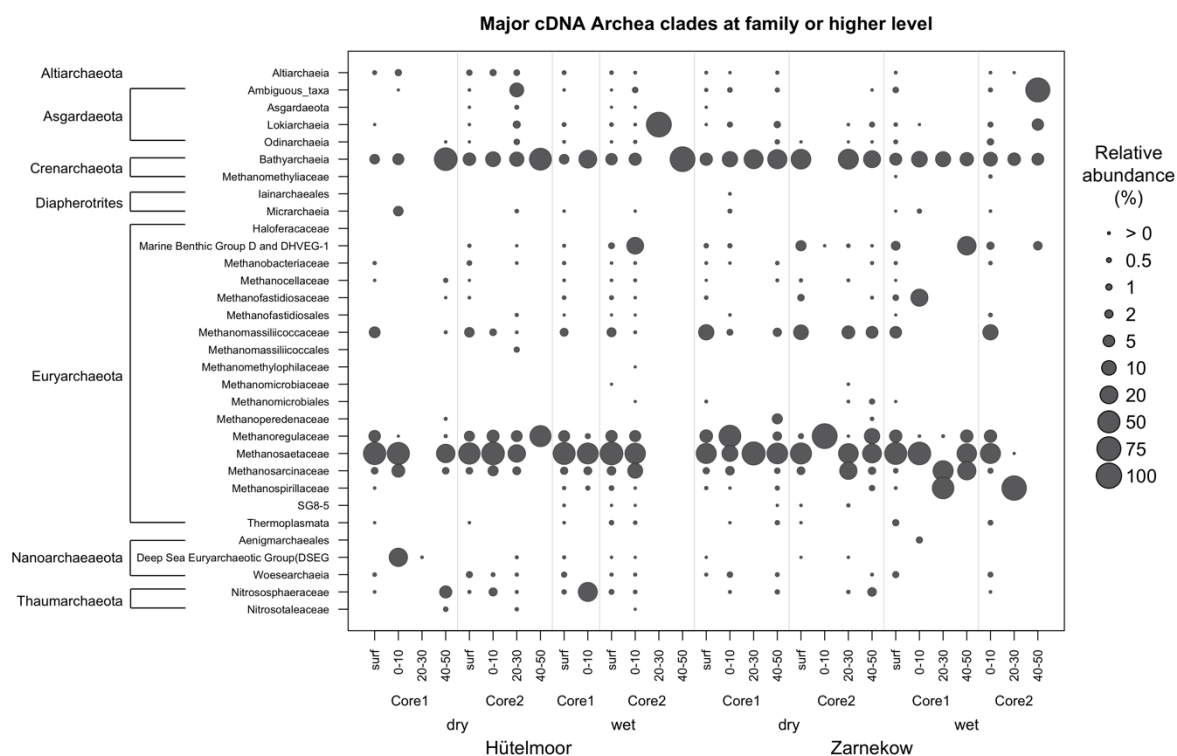


Figure S5. Bubble plots showing relative abundance of major active archaeal families during the 2018 summer drought based on cDNA sequencing. Samples are arranged along the x-axis according to site (HM and ZN for the Hütelmoor and Zarnekow, respectively) and depth section in cm given as a range (surf = surface samples). The Abbreviations DU and WU denote samples from dry unvegetated and wet unvegetated subsites, respectively. Taxa were placed at the next possible higher taxonomic level if assignment to the family level was not possible.

Table S1. Sums, means, and maximums in CH₄ emissions for the years 2015–2017 (non-drought years) and 2018 (a drought year) in the Hütelmoor, a coastal fen in northeastern Germany. Values were calculated for three distinct: the entire year, March–November, and September–December (when the drought effects were most prominent).

Year	Time period	Sum (g CH ₄ m ⁻² year ⁻¹)	Mean (g CH ₄ m ⁻² day ⁻¹)	Max (g CH ₄ m ⁻² day ⁻¹)
2015	entire year	67.3	0.18	0.74
2016	entire year	75.3	0.21	0.77
2017	entire year	60.9	0.17	0.52
2018	entire year	53.6	0.15	0.90
2015	March–November	62.9	0.23	0.74
2016	March–November	71.0	0.26	0.77
2017	March–November	58.5	0.21	0.52
2018	March–November	50.0	0.18	0.90
2015	September–December	16.8	0.13	0.47
2016	September–December	12.5	0.1	0.40
2017	September–December	15.0	0.12	0.36
2018	September–December	4.0	0.03	0.19

Table S2. Sums, means, and maximums in CH₄ emissions for the years 2015–2017 (non-drought years) and 2018 (a drought year) in Zarnekow, a riparian fen in northeastern Germany. Values were calculated for three distinct time periods: the entire year, March–November, and September–December (when the drought effects were most prominent).

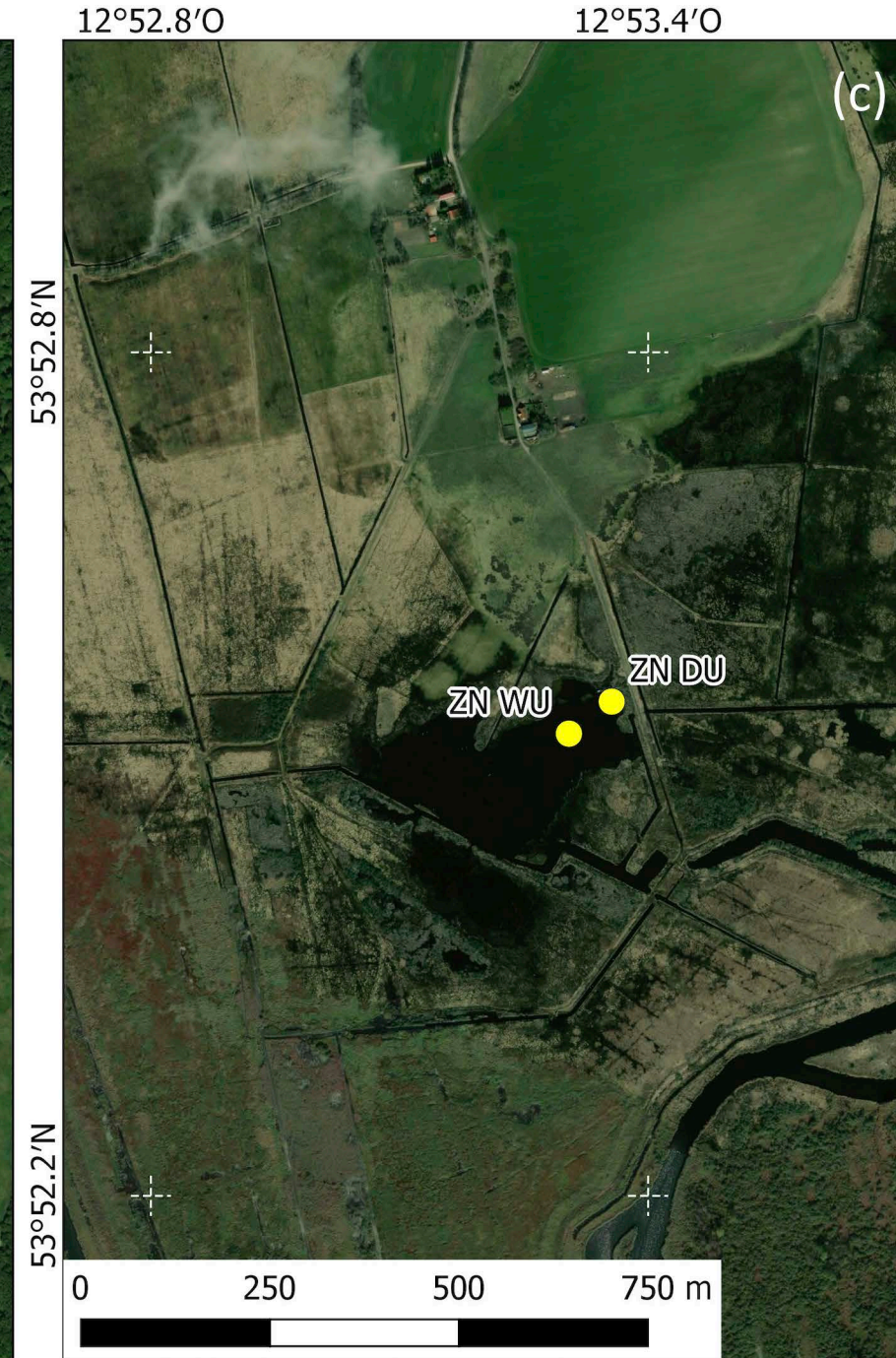
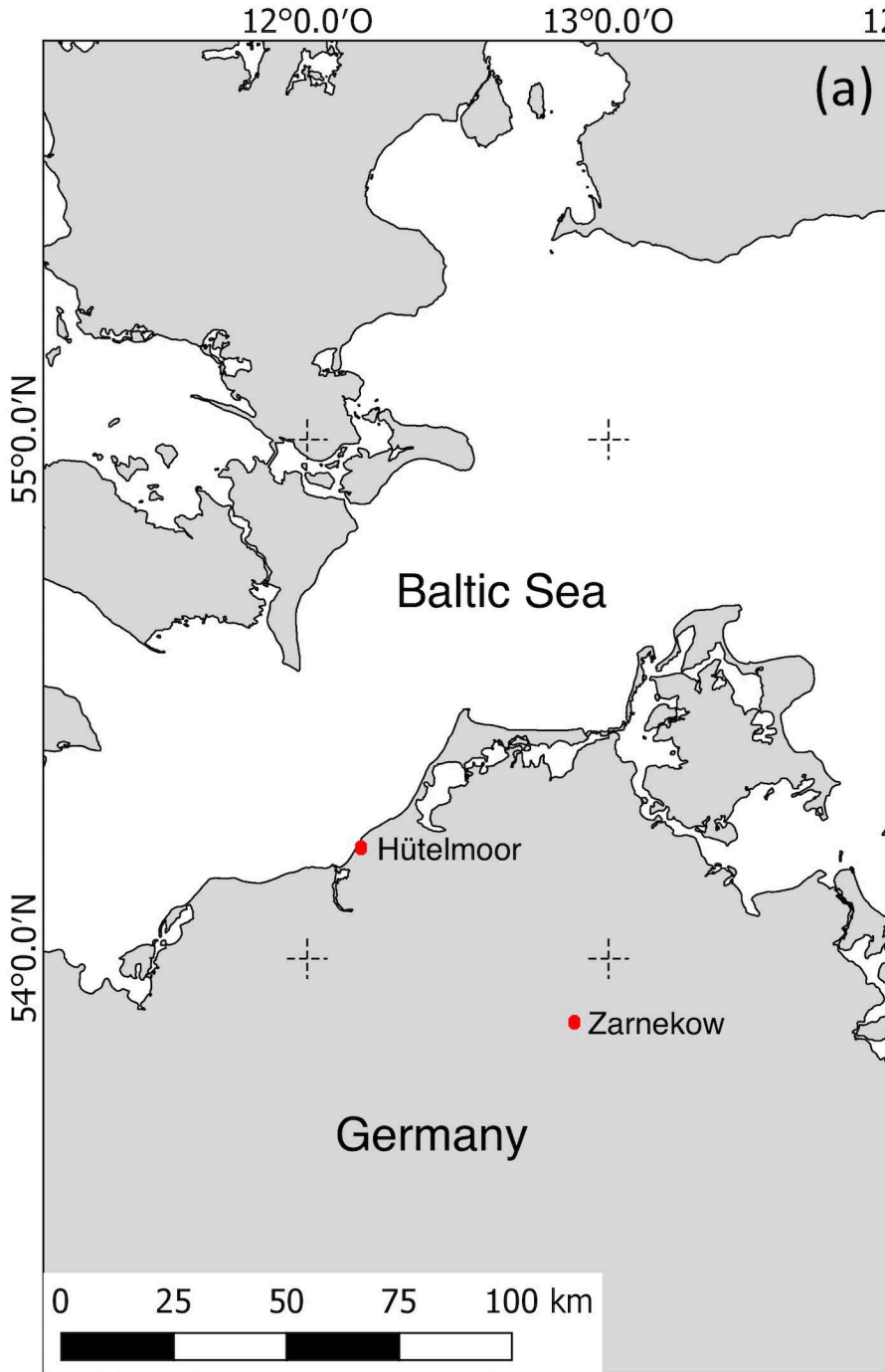
Year	Time period	Sum (g CH ₄ m ⁻² year ⁻¹)	Mean (g CH ₄ m ⁻² day ⁻¹)	Max (g CH ₄ m ⁻² day ⁻¹)
2015	entire year	39.7	0.11	0.47
2016	entire year	44	0.12	0.62
2017	entire year	40.3	0.11	0.66
2018	entire year	41.4	0.11	0.86
2015	March–November	38.6	0.14	0.47
2016	March–November	43.1	0.15	0.62
2017	March–November	39.5	0.14	0.66
2018	March–November	40.2	0.14	0.86
2015	September–December	5.8	0.04	0.36
2016	September–December	4.2	0.03	0.26
2017	September–December	4.4	0.03	0.14
2018	September–December	2.4	0.02	0.09

Table S3. qPCR-determined total microbial (16S), methanogen (*mcrA*), and aerobic methanotroph (*pmoA*) gene copy numbers for the Hütelmoor, a coastal fen in northeastern Germany. *p*-values lower than 0.05 % indicate significant differences in microbial abundances among the non-drought and drought years.

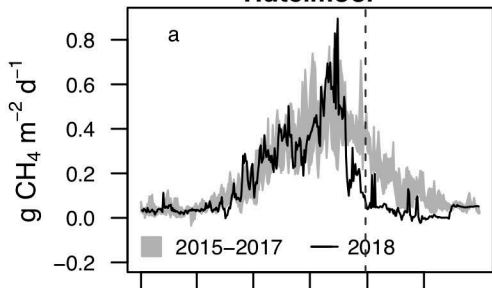
Hütelmoor	Non-drought year	Drought year	<i>p</i> -value
16S (copies g dry peat ⁻¹)	4.04 x 10 ¹⁰	2.14 x 10 ¹⁰	0.68
<i>mcrA</i> (copies g dry peat ⁻¹)	1.16 x 10 ⁹	5.05 x 10 ⁸	0.39
<i>pmoA</i> (copies g dry peat ⁻¹)	3.47 x 10 ⁷	4.11 x 10 ⁷	0.02

Table S4. qPCR-determined total microbial (16S), methanogen (*mcrA*), and aerobic methanotroph (*pmoA*) gene copy numbers for Zarnekow, a riparian fen in northeastern Germany. *p*-values lower than 0.05 % indicate significant differences in microbial abundances among the non-drought and drought years.

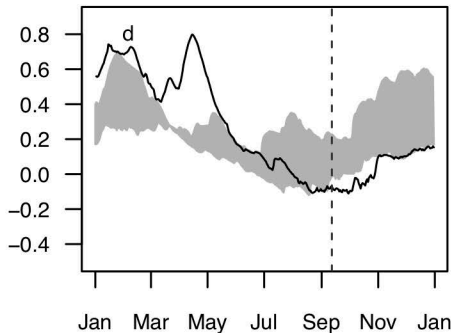
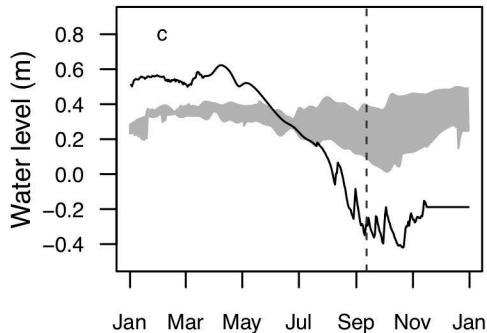
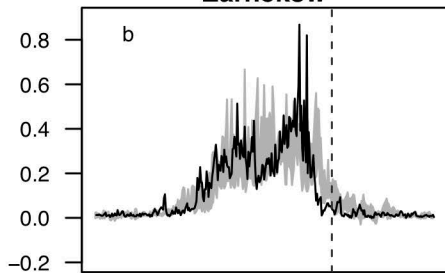
Zarnekow	Non-drought year	Drought year	<i>p</i> -value
16S (copies g dry peat ⁻¹)	6.23 x 10 ¹⁰	6.54 x 10 ¹⁰	0.03
<i>mcrA</i> (copies g dry peat ⁻¹)	8.82 x 10 ⁸	9.94 x 10 ⁷	9.8 x 10 ⁻⁵
<i>pmoA</i> (copies g dry peat ⁻¹)	4.36 x 10 ⁷	1.39 x 10 ⁷	0.15

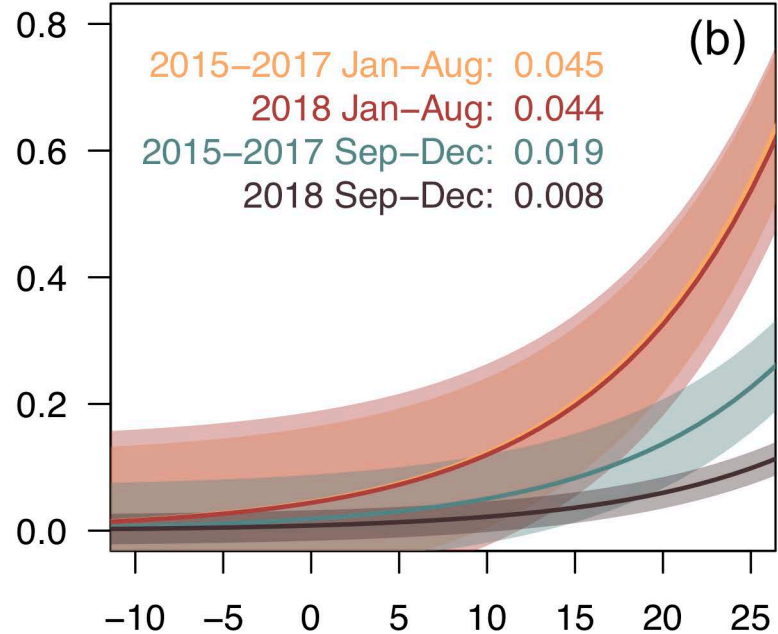
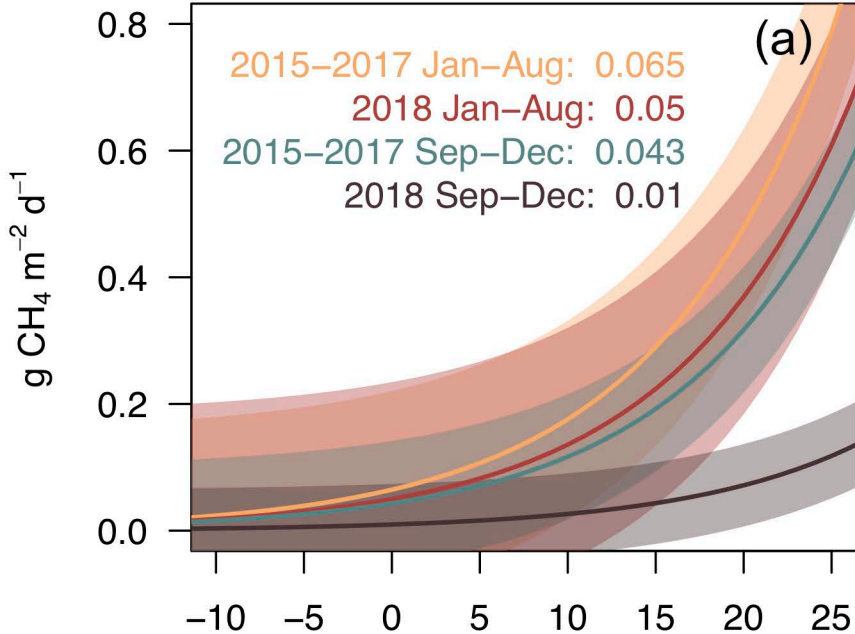


Hütelmoor

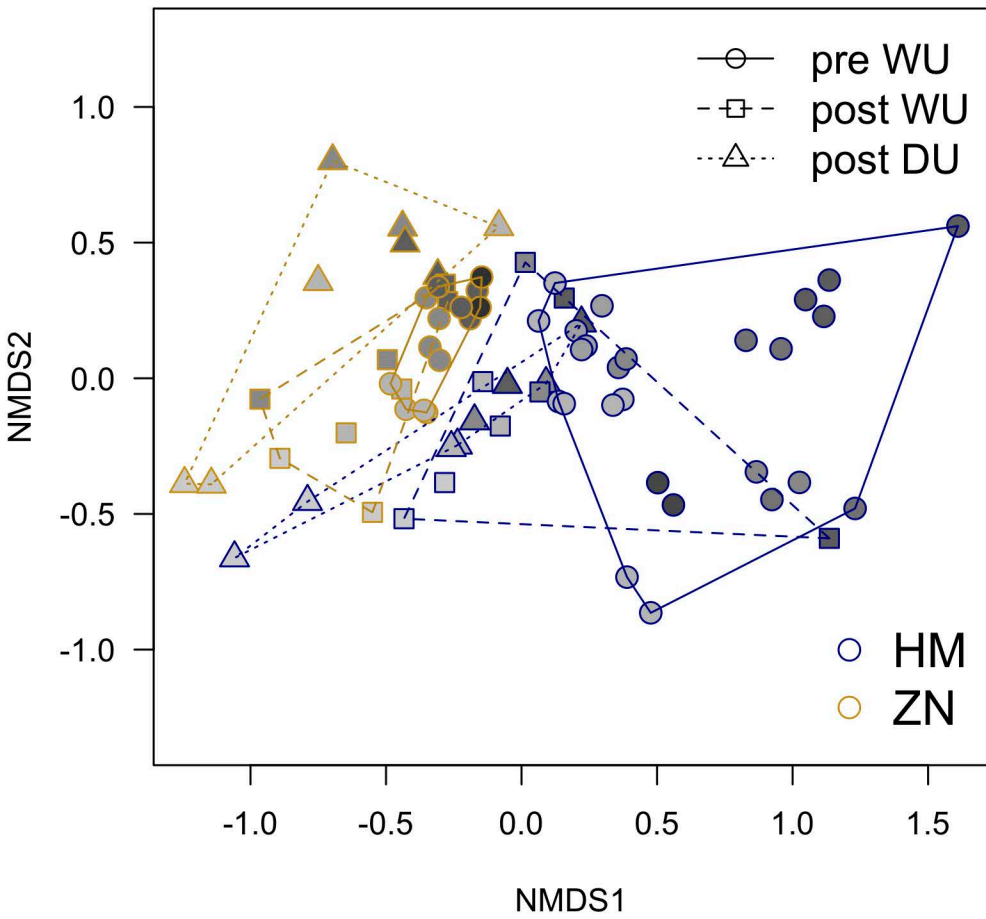


Zarnekow





Bacteria, stress = 0.13



Archaea, stress = 0.18

